Effect of previous angular deformation on flexural fatigue resistance of controlled memory nickel-titanium endodontic instruments

Bassim Aljazaeri

The University of British Columbia, Canada

Abstract

The aim of this paper was to evaluate the effect of torsional stress preloading angle on fatigue resistance of Typhoon (TYP) CM instruments. For this, TYP NiTi 25/.04, TYP NiTi 40/.04, TYP CM 25/.04 and TYP CM 40/.04 were rotated until fracture to obtain the mean angular deflection according to the +-ISO 3630-1 standard. Files were pre-torqued to 25, 50, and 75% of their elastic limit and then subjected to cyclic loading in a three-point binding device until fracture. The fatigue life was recorded for each file. The fracture surface of each fragment was examined with a scanning electron microscope. The study bore the following results - the angle of rotation at fracture of TYP CM was significantly higher than that of TYP instruments ($P < 0.05$). However, there was no significant difference between size 40 and size 25 in all types of files. The fatigue resistance of TYP CM was significantly higher than that of TYP instruments ($P < 0.05$). Size 25/.04, TYP and TYP CM files in all three preloading groups had a significantly lower fatigue life than files with no preloading ($P < 0.05$). Size 40/.04 TYP CM files in the 50% and 75% preloading groups had a significantly lower fatigue life than files in the groups with no preloading ($P < 0.05$). The fractured files in the preloading groups showed the typical pattern of fatigue failure. Conclusions: TYP CM files have a higher fatigue resistance than conventional TYP NiTi files, irrespective of the amount of previous torsional stress. Fatigue resistance of TYP CM and TYP instruments was reduced after torsional stress preloading. Size 25/.04 file fatigue life was affected by preloading at lower distortion angles than was size 40/.04 fatigue life.

Keywords: Nickel-titanium endodontic instruments, Angular deformation, Flexural fatigue resistance, Controlled memory

Introduction

'Nitinol' (NiTi) is a nearly equiatomic intermetallic alloy of nickel and titanium. The commercial Its properties of shape memory and supereslasticity result from the phase transformation between an austenitic (parent) phase [with a simple cubic B2 (CsCl) structure] to a martensite (daughter) phase (with a monoclinic B19′ structure) (Otsuka & Ren 2005). Walia et al. (1988) found that size 15 files, made by superelastic nitinol orthodontic wire, had 2-3 times the elastic flexibility in bending and torsion, as well as superior resistance to torsional fracture when compared to similar stainless-steel instruments.

Superelasticity is associated with the occurrence of a phase transformation of the alloy upon application of stress above a critical level, which takes place when the ambient temperature is above the so-called austenite-finish temperature of the material. This stress-induced martensitic transformation reverses spontaneously upon release of the stress such that the material returns to its original shape and size (Saburi 1998). This special property manifests as an enhanced elasticity of the NiTi alloy, allowing the material to recover after large strains (or distortion). The superelasticity of NiTi allows deformations of as much as 8% strain to be fully recoverable, in

comparison with a maximum of less than 1% with other alloys such as stainless-steel (Thompson 20002) (Fig.1.1). NiTi endodontic instruments with superelasticity have gained extensive popularity amongst clinicians due to their higher flexibility and greater torsional resistance compared with traditional instruments made of stainless-steel (Walia et al. 1988, Thompson 2000).

While root canal treatment has benefitted from the introduction of rotary NiTi instruments, their separation during use has been a concern to clinicians (Pruett et al. 1997, Sattapan et al. 2000, Parashos et al. 2004, Shen et al. 2006, Cheung 2007). NiTi instruments have undergone a design revolution such that instruments now can cut effectively while exhibiting resistance to fracture, even in the most challenging anatomical confines. The mechanical behavior of NiTi alloy is determined by the relative proportions and characteristics of the microstructural phases. Heat treatment (thermal processing) is one of the most fundamental approaches toward adjusting the transition temperatures of NiTi alloys (Frick et al. 2005, Gutmann & Gao 2012) and affecting the fatigue resistance of NiTi endodontic files.

Figure 1.1 NiTi phase transformation. (IEJ 2000:297-310)

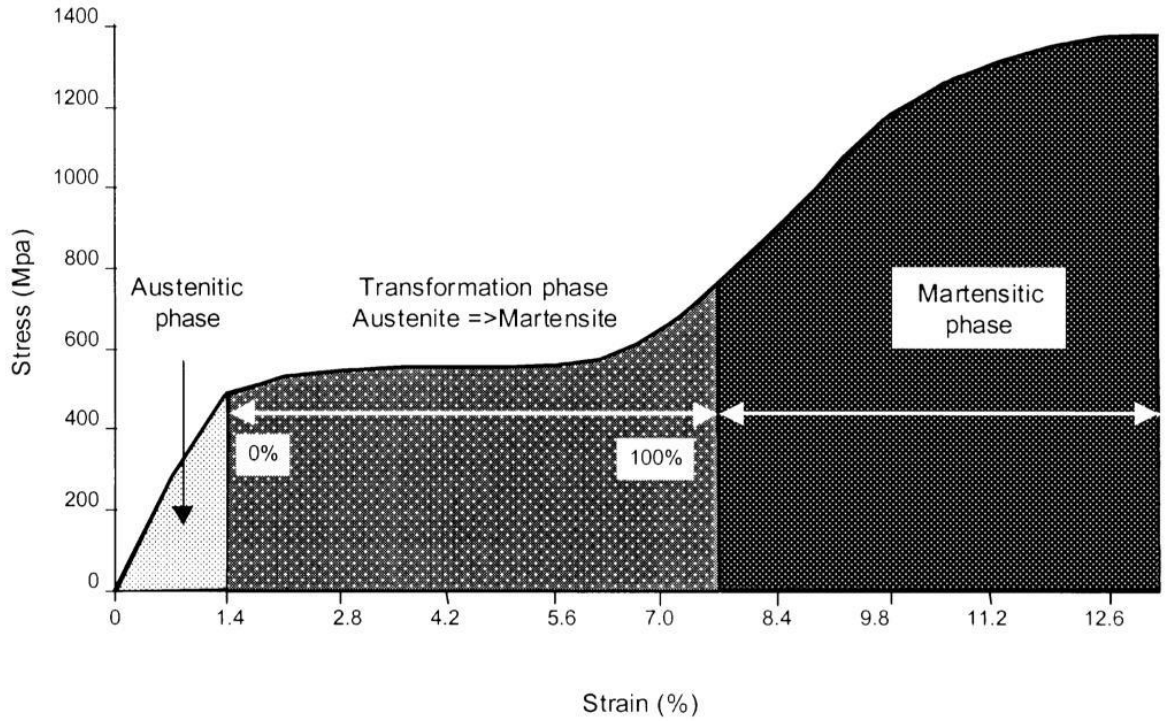

NiTi alloy has three distinct microstructural phases: austenite, martensite, and R-phase. The martensite phase's crystal structure (known as a monoclinic, or B19' structure) has the unique ability to undergo limited deformation in some ways without breaking atomic bonds. This type of deformation is known as twinning, which consists of the rearrangement of atomic planes without causing slip, or permanent deformation. During this deformation, the maternsite is able to undergo about 6–8% strain. When martensite is reverted to austenite by heating, the original austenitic structure is restored, regardless of whether the martensite phase was deformed. Thus, ‘shape memory’ refers to the fact that the shape of the high temperature austenite phase is

'remembered', even though the alloy is severely deformed at a lower temperature. Traditional superelastic NiTi files are in austenite phase at body temperature. However, CM NiTi files are in a mixture of austenite and martensite phases at body temperature. The martensitic phase of NiTi has some unique properties that have made it an ideal material for many applications (Davis 2000). The martensitic phase transformation has excellent damping characteristics because of the energy absorption characteristics of its twinned phase structure. Compared with austenite, the martensite favors reducing the risk of file fracture under high stress because it can be plastically deformed rather than broken. On the other hand, the martensitic form of NiTi has remarkable fatigue resistance. The instruments of martensite phase can be easily deformed, yet they will recover their shape on heating above the transformation temperatures. Instruments made from CM Wire (TYP CM and DSSS0250425NEYY CM [NEYY CM]) were nearly 300%–900% more resistant to fatigue failure in a 3-point bending device than instruments made from conventional NiTi wire with the same design in a dry environment (Shen *et al*. 2011a) as well as under various other conditions (Shen *et al*. 2012a) in a 3-point bending device.

Peters *et al*. (2012) evaluated torsional and fatigue limits, as well as torque during canal preparation of HyFlex (CM wire) instruments. They found that HyFlex rotary instruments are bendable and flexible and have similar torsional resistance compared to instruments made of conventional NiTi. Fatigue resistance is much higher, and torque during preparation is less, compared to other rotary instruments tested previously under similar conditions.

Figure 1.2 DSC curves of the TYP and TYP CM NiTi instruments. Heating (upper) and cooling (lower) curves are shown. (JOE 2011:1566-71)

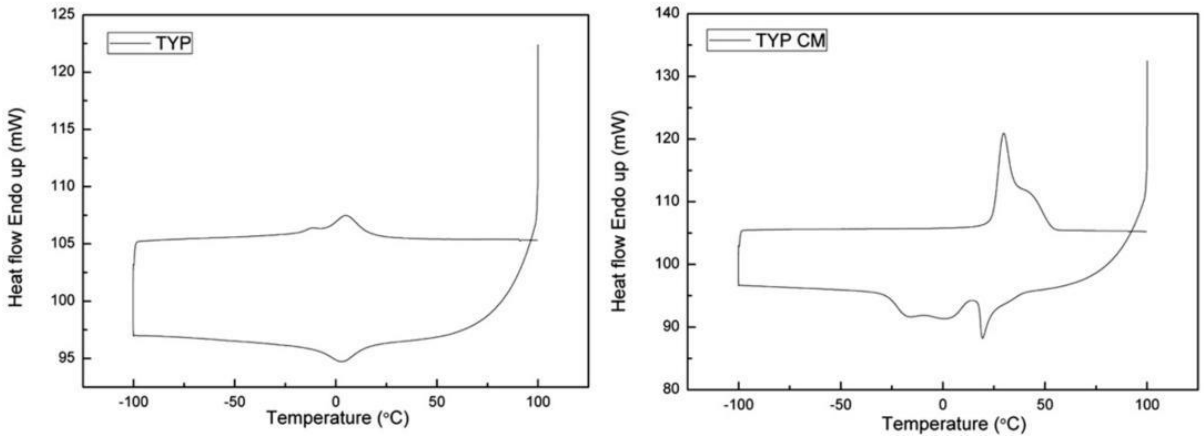

Figure 1.3 XRD patterns for NiTi TYP and TYP CM instruments at 25oC. (JOE 2011:1566-71)

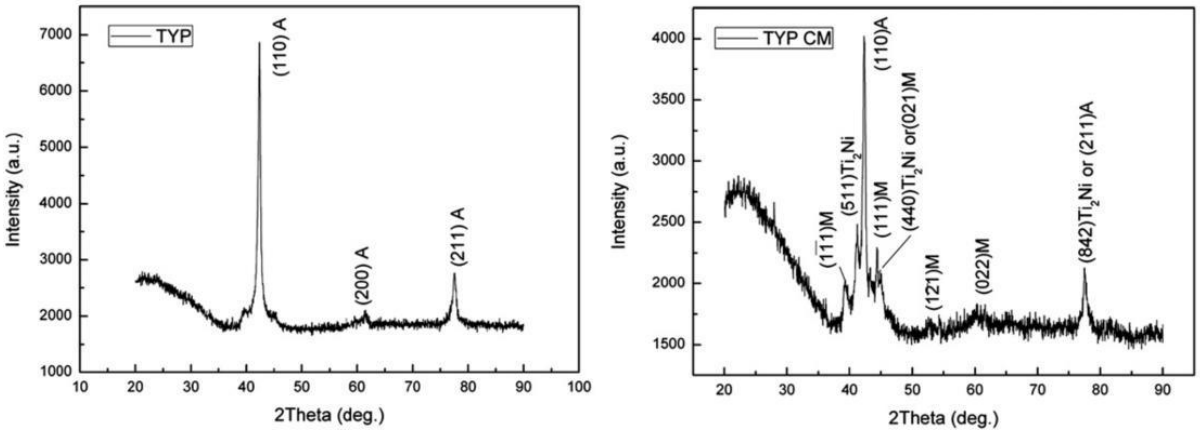

Figure 1.4 (A) DSC curves of raw and heat-treated (HT) SE and CM wires with diameter of 1.22 mm. (B) DSC curves of raw SE wires with diameter of 1.22 mm and 0.64 mm. (C) Tensile stress-strain curves of raw CM and SE wires with diameter of 1.22 mm. Test was conducted at room temperature and oral temperature (37oC). (D) Tensile stress-strain response of SE and CM wires during loading-unloading process performed at room temperature. (E) Flexural load-deflection curves of raw SE wires. (F) Flexural load-deflection curves of raw CM wires. Tests were conducted at room temperature (RT, 23oC ± 2oC), oral temperature (37oC), and 60oC. (JOE 2012; 1535-40)

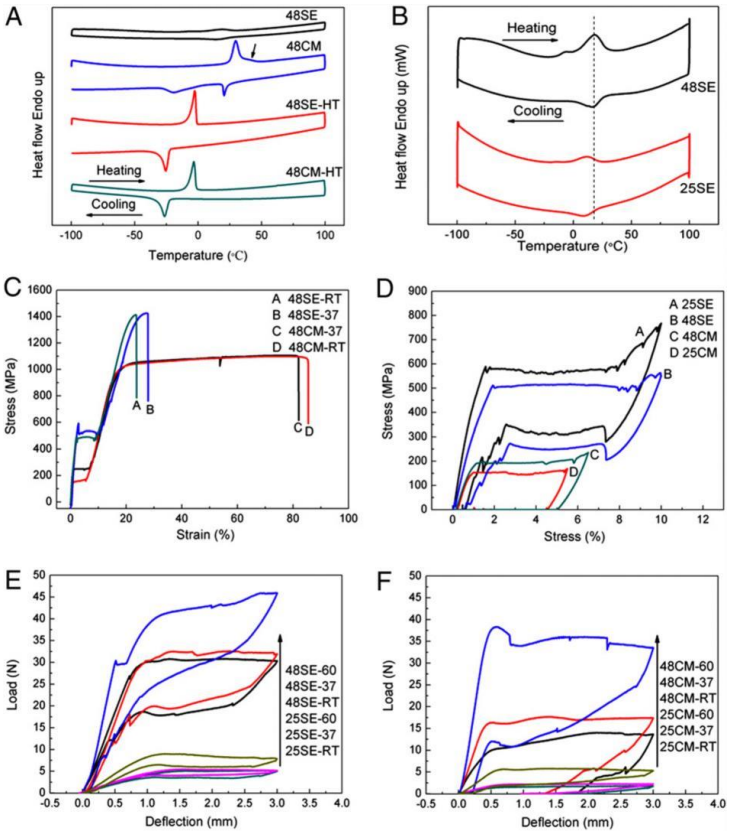

Instrument Fracture

It has been reported that fracture of a NiTi instrument may occur from either torsional or flexural fatigue or a combination of the two (Sattapan *et al*. 2000; Cheung *et al*. 2005; Wei *et al*. 2007). The incidence of conventional superelastic NiTi instrument fracture in clinical practice for files used multiple times has varied from 3% to 21% (Sattapan *et al*. 2000, Parashos *et al*. 2004, Peng *et al*. 2005, Alapati *et al*. 2005, Shen *et al*. 2006). Although fractured instruments may not compromise the outcome if the treatment is performed to a high standard (Spili *et al*. 2005), the retained file fragments may impede microbial control beyond the obstruction.

All of the previous studies attempted to simulate an instrument rotating with a curvature and then determine how long such an instrument would last before fatigue fracture occurred. Theoretically, the device for fatigue tests should confine the rotary file into a precise trajectory, in terms of the radius and angle of the curvature and the location of the maximum curvature.

The measurement of the torsional strength of root canal instruments is typically performed in a torsiometer according to the procedure described by the American Dental Association specification #28 (ANSI/ADA Specification No. 28, 2002). The ISO/ANSI specifications have prescribed a test method for (stainless-steel) root canal reamers and files in which 3mm of the tip of the instrument is rigidly fixed and subjected to twisting in a clockwise or a counterclockwise direction A wide variety of rotary NiTi instruments have been tested in this manner. However, torsional failure due to such a monotonic condition rarely occurs clinically. Both the ADA method (ANSI/ADA Specification No. 28, 2002) and ISO protocol #3630-1 (International Organization for Standardization 2008) only simulate torsional bending in straight canals, as the torque is measured in relation to the rotation axis. However, rotary instruments are subject to varying loads in actual clinical situations, with fractures likely to be the result of a combination of repetitive flexural and torsional stresses.

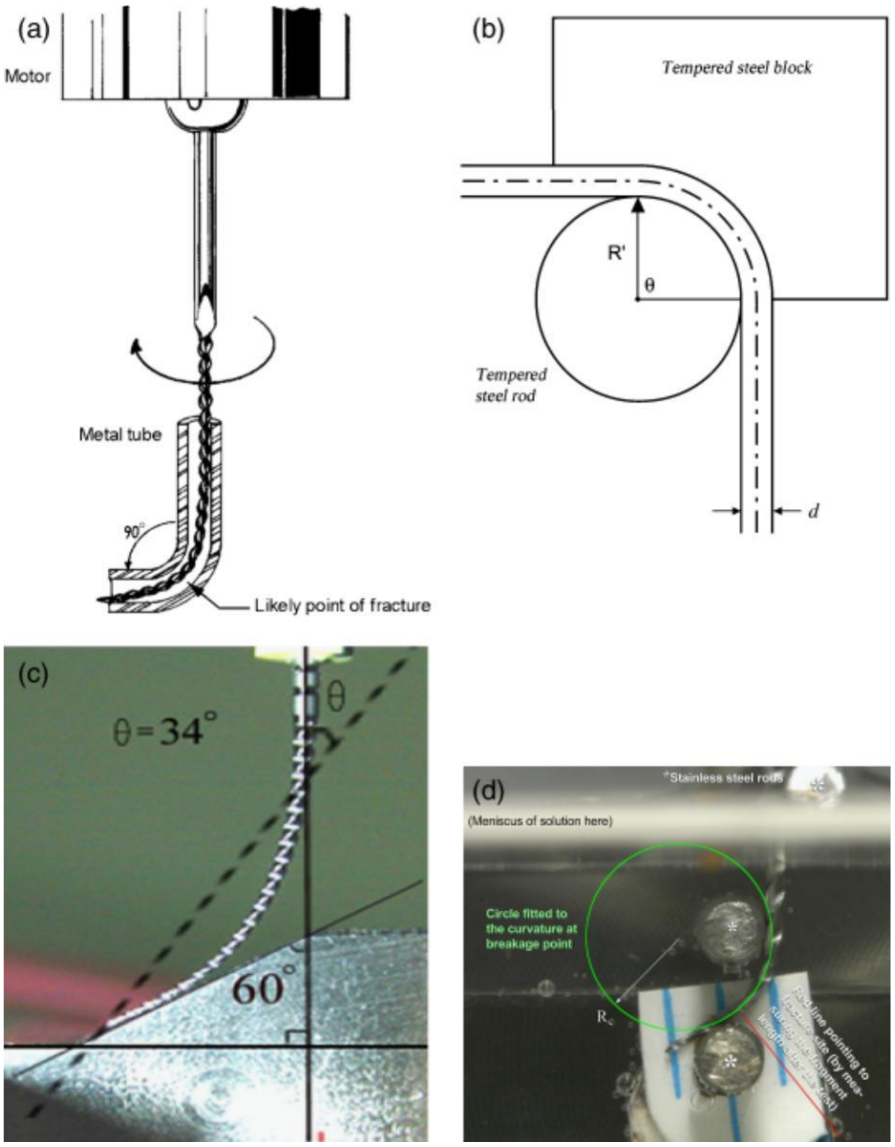

Methodology

Sample Preparation

TyphoonTM (Clinician's Choice Dental Products, New Milford CT) rotary endodontic files were selected for this study because the same cross sectional design was found in both the NiTi and CM files (Fig. 1.2).

To evaluate the effect that torsional preloading may have on cyclic fatigue, torsional preloading was done on the files under three conditions. Twelve (12) unused instruments in each group were exposed to either 25%, 50%, or 75% of their respective mean distortion angle at torsional fracture (Table 3.1). After preloading to various extents, fatigue tests were performed to measure the fatigue life.

Torque Preloading

The torsion tests were performed based on International Organization for Standardization ISO 3630-1 (International Organization for Standardization, 2008) using a torsion machine: 3 mm of the instrument tip was secured firmly in a specifically designed soft brass holder. The apparatus was composed of a torque sensor (Futek Model TFF 400, Futek, CA, USA) and a low-speed rotating motor (Fig. 2.2). The instrument's shank was then rotated at 2 rpm until fractures occurred. Before testing, each instrument handle was removed at the point where the handle is attached to the shaft. The end of the shaft was clamped into a chuck connected to a reversible geared motor. The torsional load and distortion angular were recorded until the instrument broke (Ullmann & Peters 2005; Gao et al. 2012; Lopes et al. 2013, Campbell et al. 2014).

Method to Cyclically Fatigue Files

For the determination of resistance to cyclic fatigue, unused size 25/.04 and size 40/.04 TYP and TYP CM instruments (n = 12 in each group) were placed in a 3-point bending apparatus with a 14 mm radius and 45° curve in deionized water (Shen et al. 2011a & 2012a) (Fig. 2.3). Briefly, each NiTi instrument was constrained to a curve by 3 rigid, stainless-steel pins; a calibrated digital photograph of the curvature was taken. Only a 16-mm length from the tip of the instrument was immersed in deionized water at the temperature of 23 ± 2 oC. The instruments were then rotated at 500 rpm until fracture occurred to determine baseline scores (Table 3.2). The fatigue life, or the total seconds to failure, was recorded.

Fractographic Examination

The fracture surfaces of all fragments were examined under a scanning electron microscope (SEM; Stereoscan 260; Cambridge Instruments, Cambridge, UK). In instruments that failed due to fatigue only, the number of crack origin(s) for each specimen was recorded. The region in which the dimple area could be found was outlined on the photomicrograph for fatigue failure groups, and measured with ImageJ 1.4 g software (National Institutes of Health, Bethesda, MD) on each photomicrograph (Shen et al. 2011a & 2012a).

Statistical Analysis

The results were analyzed with a two-way ANOVA and post hoc analysis using software (SPSS for Windows 11.0, SPSS, Chicago, IL) at a significance level of $P < 0.05$.

Figure 2.1 TYP CM NiTi instruments. The working parts of the files have been bent into specific curved positions, which is not possible with conventional superelastic NiTi files.

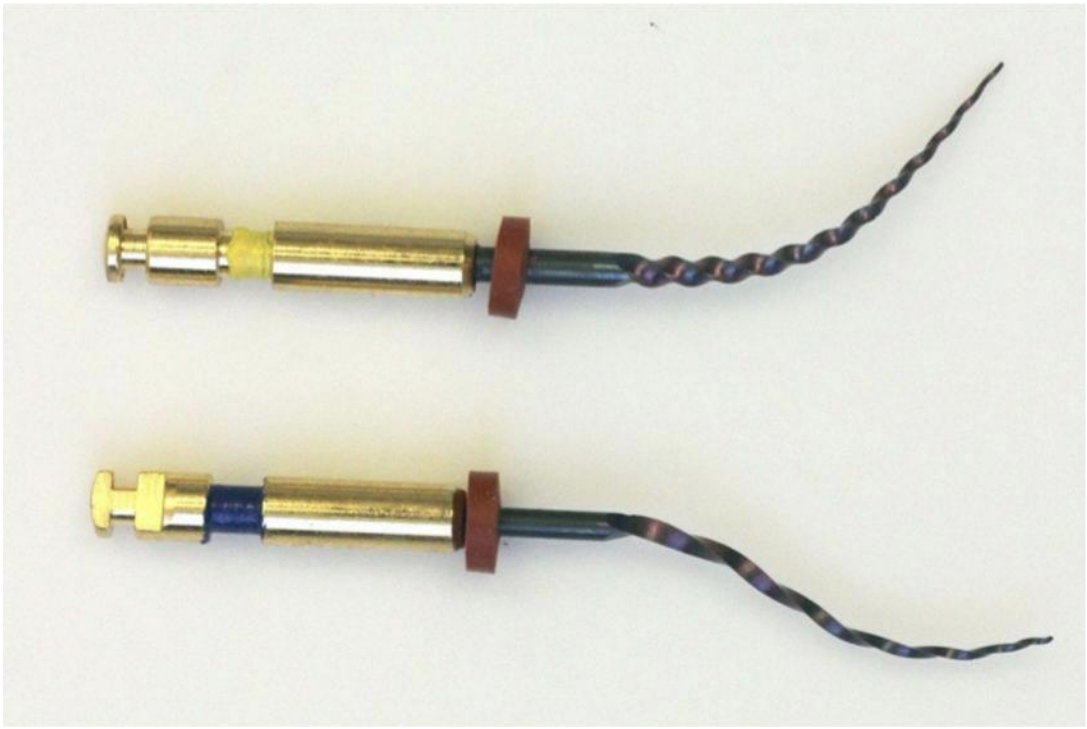

Figure 2.2 Torsional test for NiTi TYP and TYP CM instruments. (Courtesy Y. Shen)

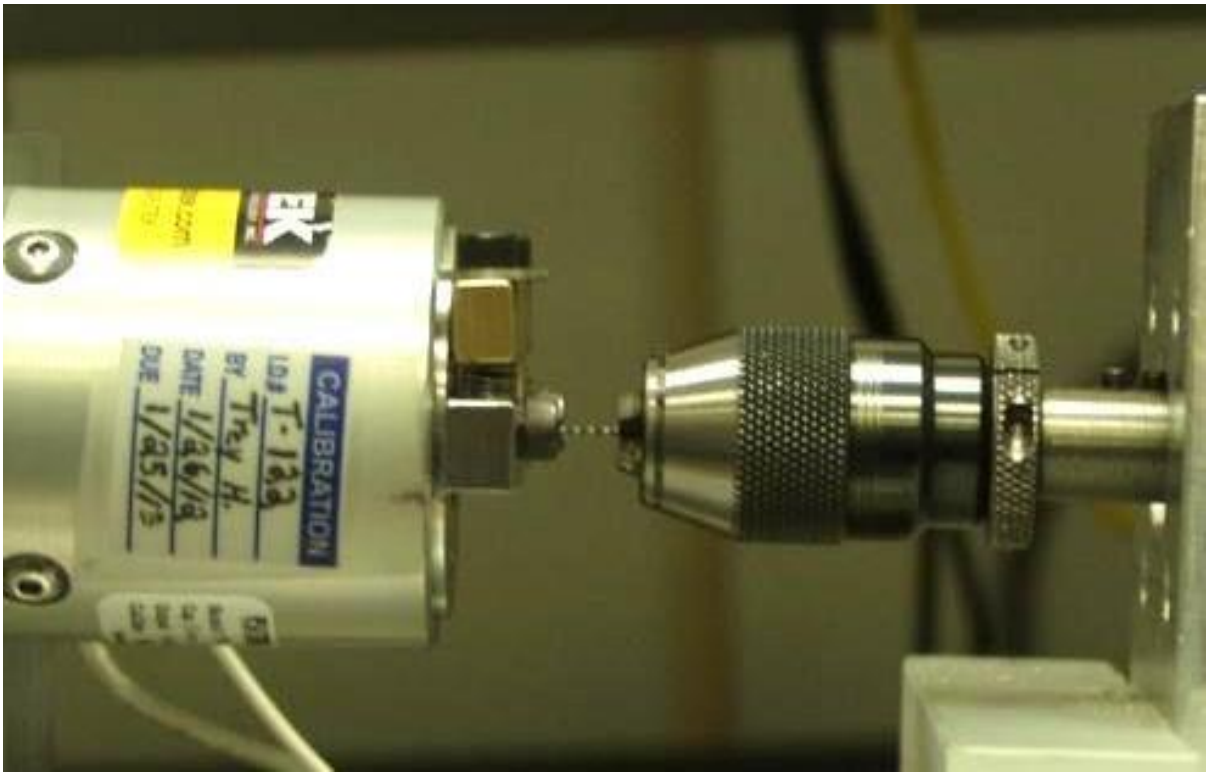

Figure 2.3 Three-point bending apparatus for fatigue tests of NiTi TYP and TYP CM instruments.

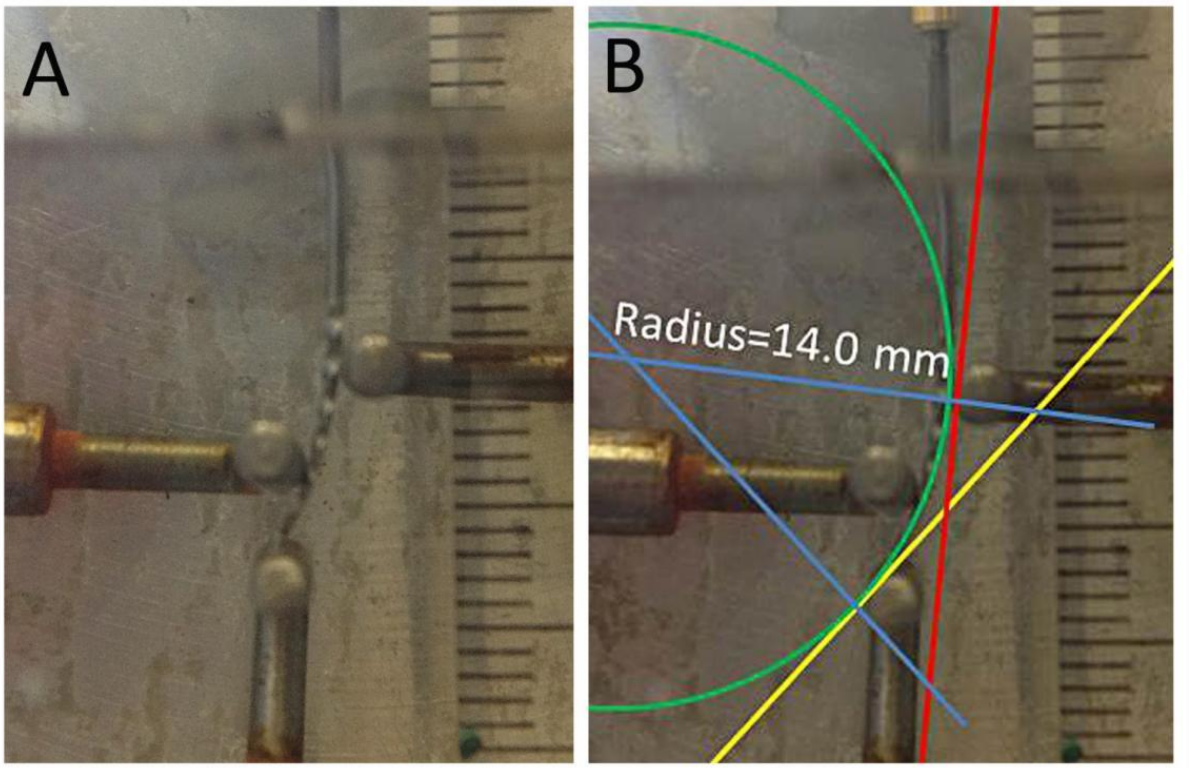

Results and Discussion

The angle of rotation at fracture of TYP CM was significantly higher than that of TYP instruments (two-way ANOVA; $P < 0.05$) (Table 3.1). However, there was no significant difference between size 40 and size 25. The fatigue resistance of TYP CM was also significantly higher than that of TYP instruments (two-way ANOVA; $P < 0.05$)(Table 3.2). Size #25 files had a higher fatigue resistance than size #40 files (post hoc analysis; $P < 0.05$).

TYP and TYP CM size 25 files preloaded with torsional stress had a significantly lower fatigue life than files in the groups without preloading (post hoc analysis; $P < 0.05$) (Table 3.2), even with a small amount torsional preloading. There was no significant difference in fatigue resistance among the 25%, 50% and 75% preloading groups. In size 40/.04, TYP CM files in the 50% preloading group had a significantly lower fatigue life than files without preloading (post hoc analysis; $P < 0.05$). However, there was no significant difference in fatigue resistance of conventional TYP file size 40 with or without preloading.

There was little difference in the longitudinal or lateral view between new and 25% torsionally preloaded TYP files (Fig. 3.1 & 3.2): the lateral aspect of the preloaded file did not show any specific topographic features. In TYP CM size 25 and 40 only some files had a slight plastic deformation after 25% torsional preloading (Fig. 3.3). In the 50% torsionally preloaded group, plastic deformation occurred in size 25 and 40 TYP CM files as well as in TYP size 25 files (Fig. 3.4 - 3.6). After 75% torsional preloading, all files had plastic deformation 2-4 mm away from

the instrument tip in the lateral view (Fig. 3.7 - 3.11). There were numerous microcracks on the plastic deformation area (Fig. 3.7 - 3.11). Of particular interest, the microcracks did not seem to follow the machining grooves on the instrument surface, but rather ran irregularly (Fig. 3.7 - 3.11). The length of the fractured piece ranged from 2.7 - 3.3 mm.

Fractographically, in instruments failed by fatigue only or fatigue after torsional loading, the crack origins and areas showing microscopic fatigue-striations and dimple rupture could be identified on all fracture surfaces (Fig. 3.13 - 3.24). Most TYP NiTi instruments (10/12 for size 25 and 9/12 for size 40) had a single crack origin, while TYP CM files had a higher number of multiple crack origins than TYP files. The areas occupied by the dimple region of the total surface area of the fractured cross-sections in size 40 files were significantly larger in TYP instruments than in TYP CM (Fig. 3.23) files without preloading (70.7 ± 12.1 for TYP *vs*. 24.6 ± 9.8 for TYP CM) and files preloaded with torsional stress (71.6 ± 10.7 for TYP *vs*. 22.5 ± 11.2 for TYP CM) ($P < 0.05$). In TYP files size 25, the areas occupied by the dimple region of the total surface area of the fractured cross-sections files in without preloading were slightly larger (35.2 ± 9.9) than in TYP CM files (18.9 ± 8.2) (Fig. 3.24). There was no significant difference between TYP files with (30.7 ± 8.2) and without preloading (35.2 ± 9.9). The fractography corresponded to the torsional failure and showed the torsional fracture pattern with circular abrasion marks and skewed dimples near the center of rotation (Fig. 3.25).

Table 3.1 The distortion angles (in degrees) of files (mean ± S.D.) subjected to 25%, 50% and 75% of the average maximum angular deflection until the file broken. Different superscripts letters indicate a statistically significant difference at $P < 0.05$ (post hoc analysis)

Files	N	The average maximum angular deflection at torsional fracture (°)	The percentage of the average maximum angular deflection		
			25%	50%	75%
TYP 25/.04	12	500 ± 61[a] (°)	125 (°)	250 (°)	375 (°)
TYP CM 25/.04	12	792 ± 50[b] (°)	198 (°)	396 (°)	594 (°)
TYP 40/.04	12	412 ± 37[a] (°)	103 (°)	206 (°)	309 (°)
TYP CM 40/.04	12	924 ± 108[b] (°)	231 (°)	462 (°)	693 (°)

Figure 3.1 Lateral-view scanning electron micrograph of size 25 TYP files with 25% preloading of the maximum distortion angle (A - C).

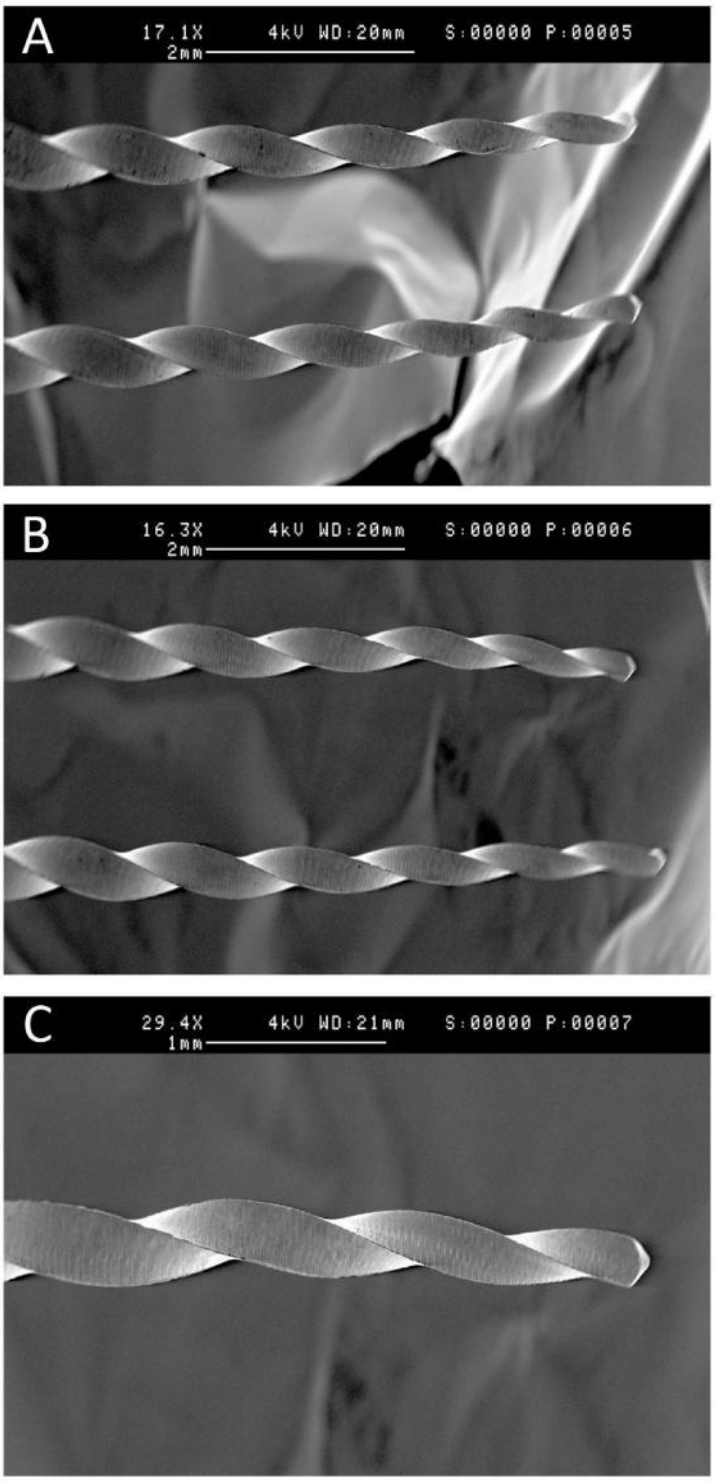

Figure 3.2 Lateral-view scanning electron micrograph of size 40 TYP files with 25% preloading of the maximum distortion angle (A); (B) high magnification view of the bottom file seen in (A); (C) high magnification view of (B).

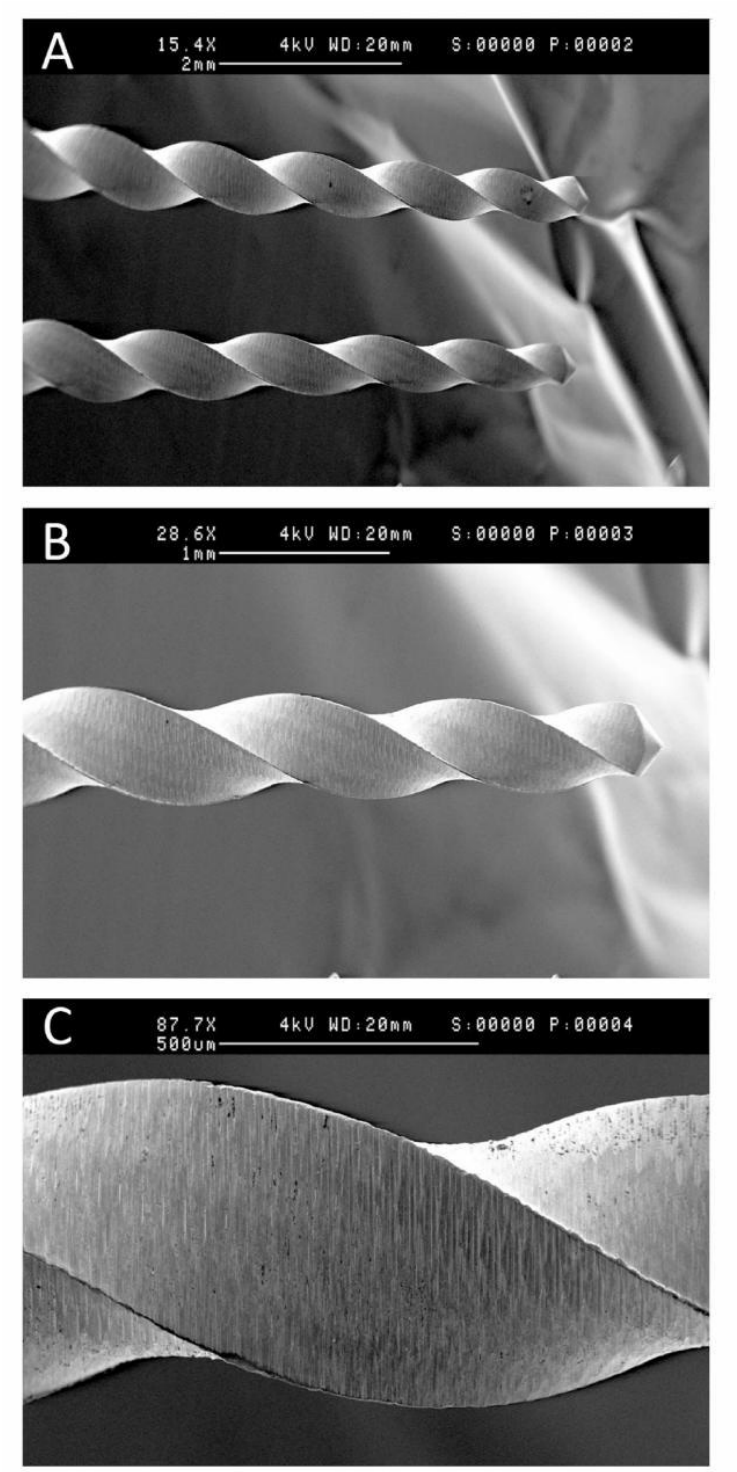

Figure 3.3 Lateral-view scanning electron micrograph of size 25 TYP CM files with 25% preloading of the maximum distortion angle (A); (B) high magnification view of (A); size 40 TYP CM files with 25% preloading of the maximum distortion angle (C); (D) high magnification view of the bottom file seen in (C).

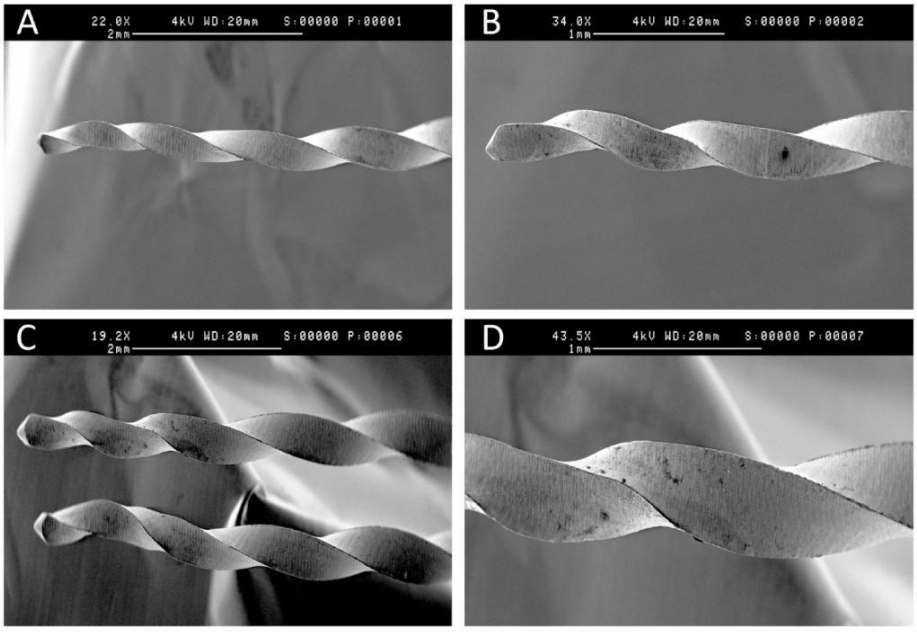

Figure 3.4 Lateral-view scanning electron micrograph of size 25 TYP files with 50% preloading of the maximum distortion angle (A); (B) high magnification view of the top file seen in (A); size 40 TYP file with 50% preloading of the maximum distortion angle (C); (D) high magnification view of (C).

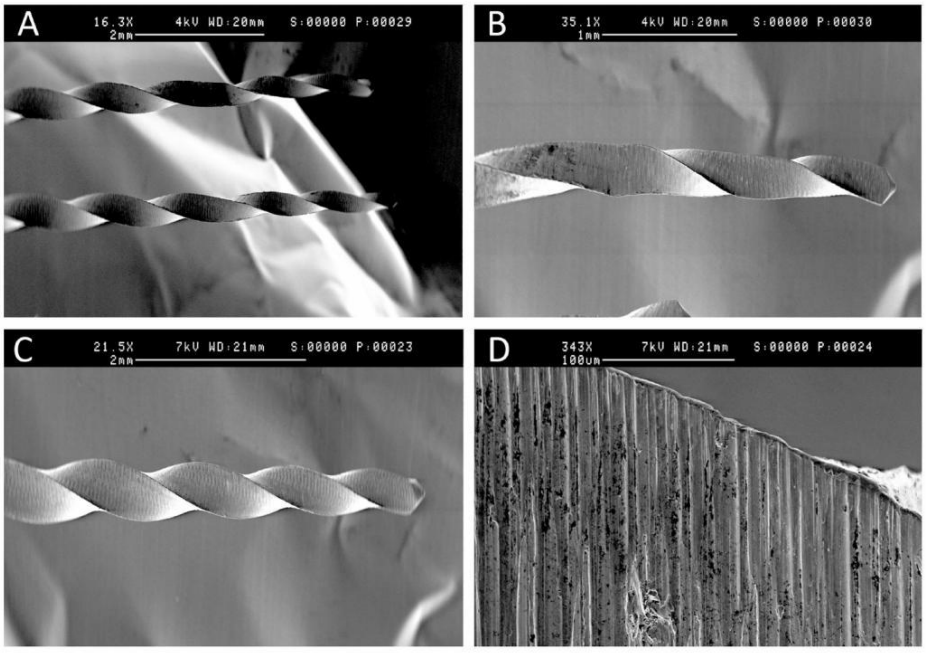

Figure 3.5 Lateral-view scanning electron micrograph of a size 25 TYP CM file with 50% preloading of the maximum distortion angle (A); (B-D) high magnification view of (A).

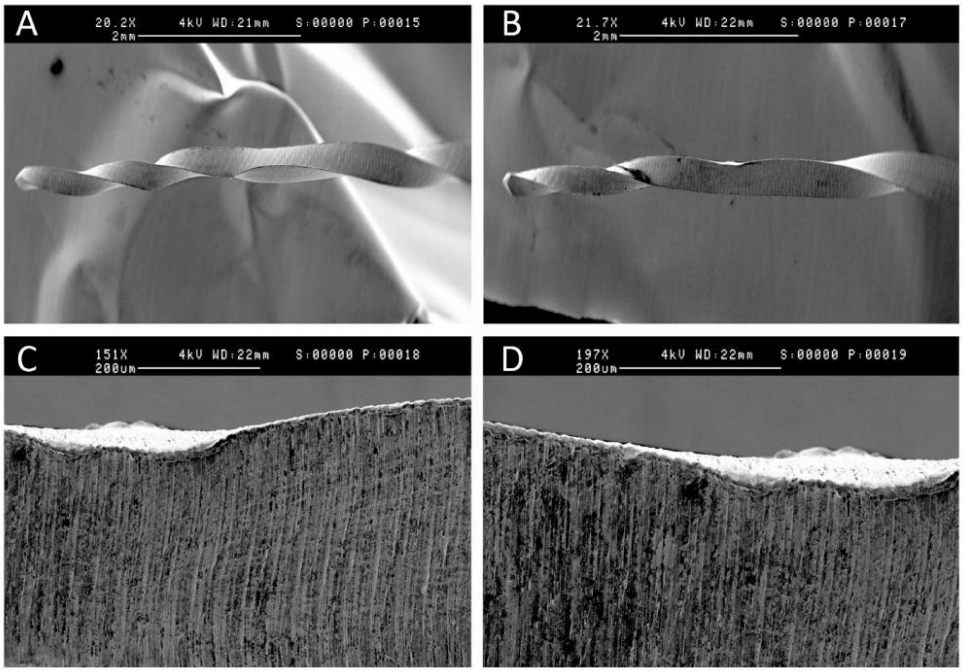

Figure 3.6 Lateral-view scanning electron micrograph of a size 40 TYP CM file with 50% preloading of the maximum distortion angle (A); (B) high magnification view of the bottom file shown in (A); (C) size 40 TYP CM file with 50% preloading of the maximum distortion angle; (D) high magnification view of (C).

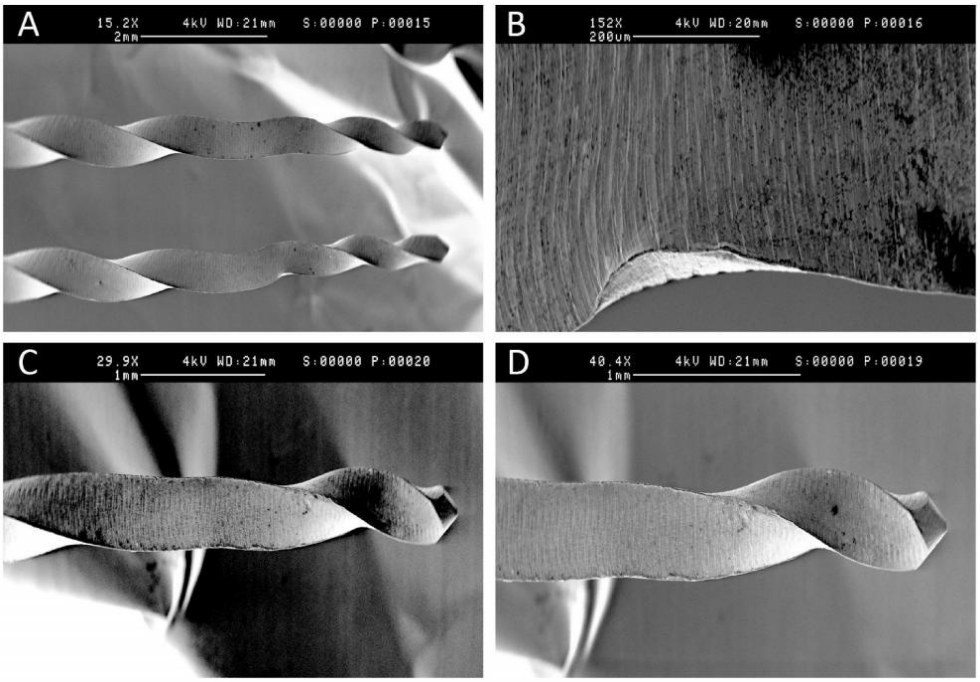

Figure 3.7 Lateral-view scanning electron micrograph of a size 25 TYP file with 75% preloading of the maximum distortion angle (A); (B-D) high magnification view of (A).

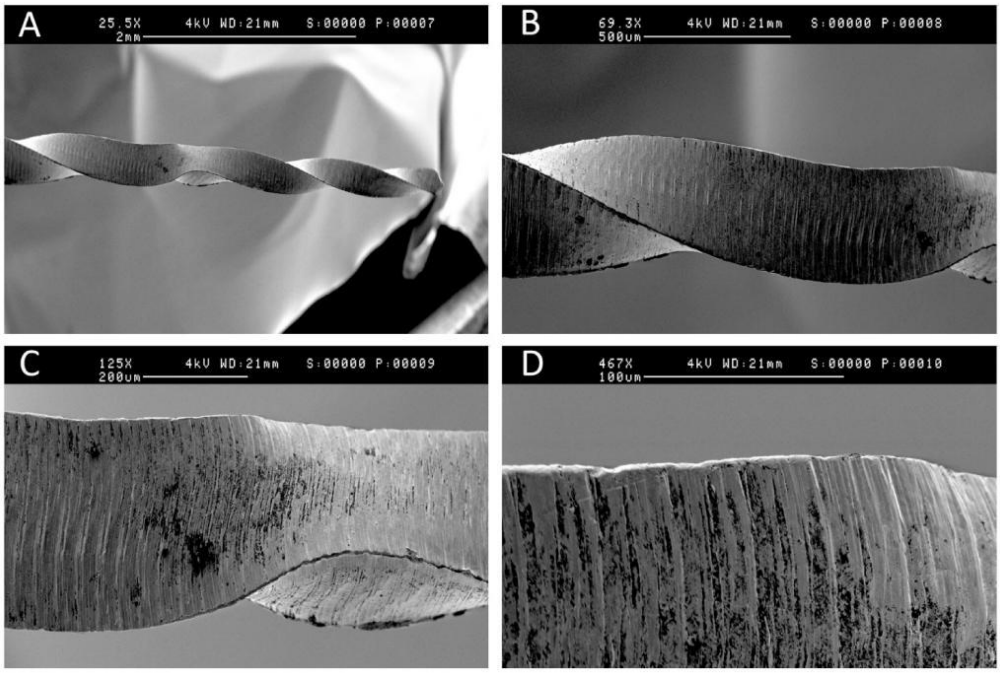

Figure 3.8 Lateral-view scanning electron micrograph of a size 40 TYP file with 75% preloading of the maximum distortion angle (A); (B-D) high magnification view of (A).

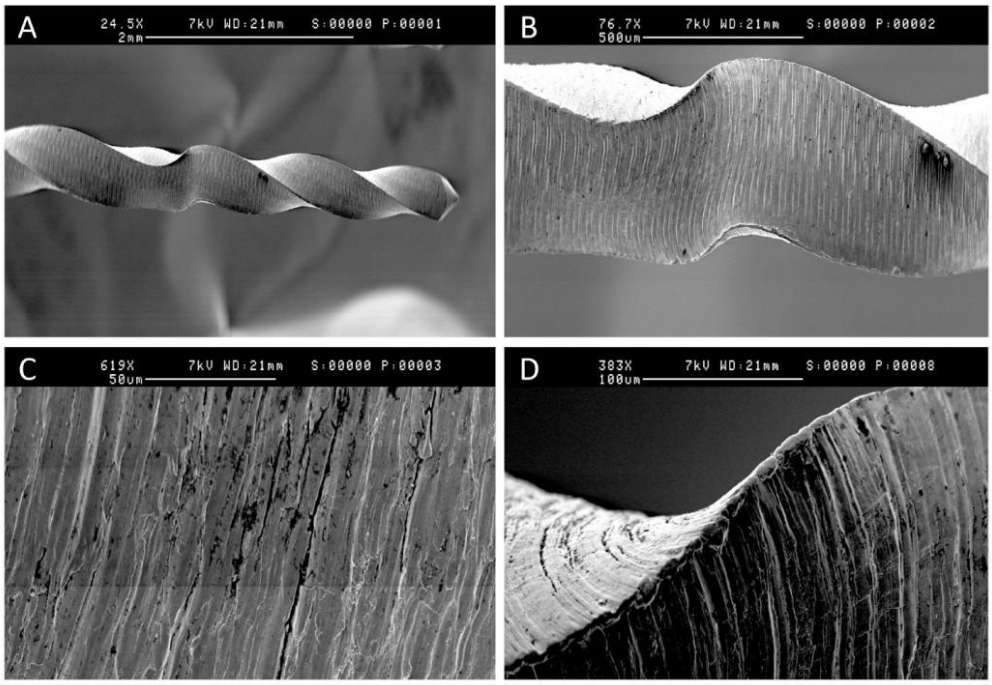

Figure 3.9 Lateral-view scanning electron micrograph of a size 25 TYP CM file with 75% preloading of the maximum distortion angle (A); (B) high magnification view of the top file seen in (A); (C & D) high magnification view of (B).

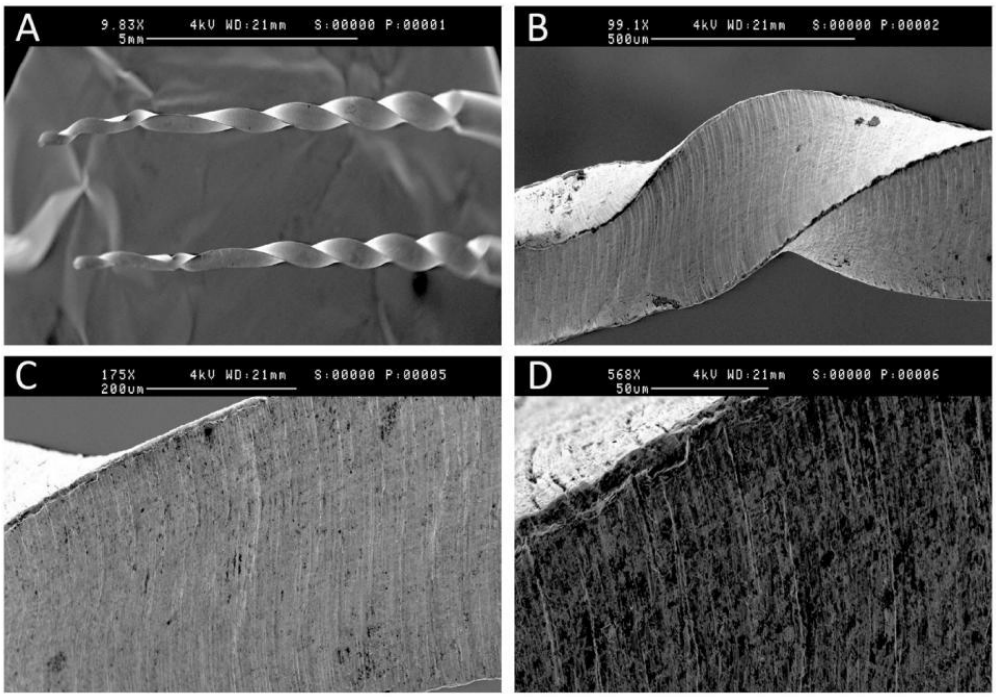

Figure 3.10 Lateral-view scanning electron micrograph of a size 25 TYP CM file with 75% preloading of the maximum distortion angle (A); (B) high magnification view of the bottom file seen in (A); (C & D) high magnification view of (B).

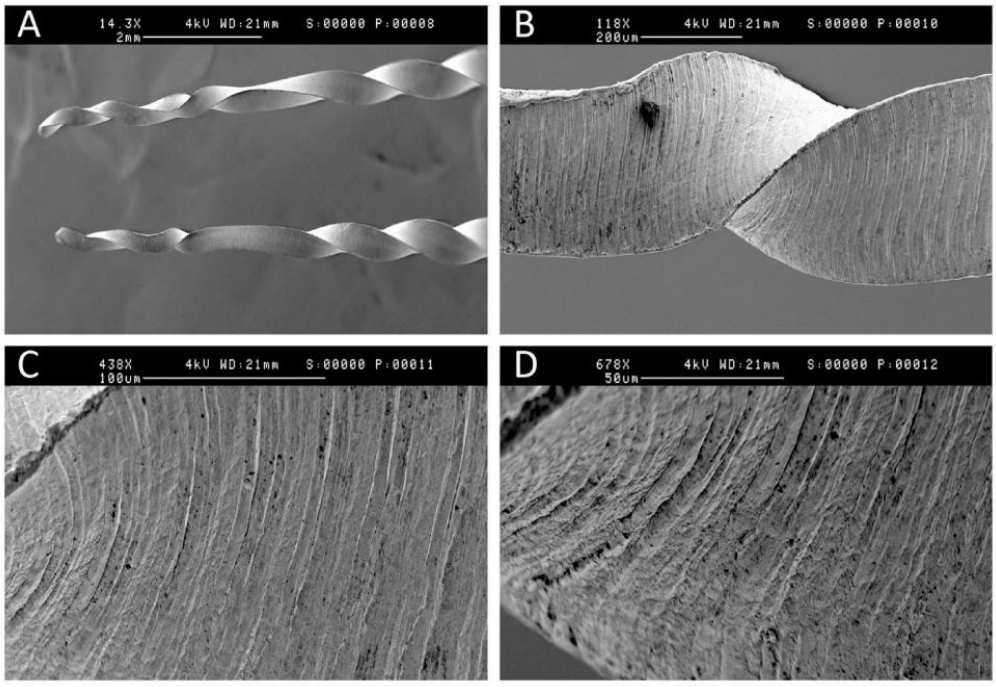

Figure 3.11 Lateral-view scanning electron micrograph of size 40 TYP CM files with 75% preloading of the maximum distortion angle (A); (B) high magnification view of the top file seen in (A); (C) high magnification view of the bottom file seen in (A); (D) high magnification view of (C).

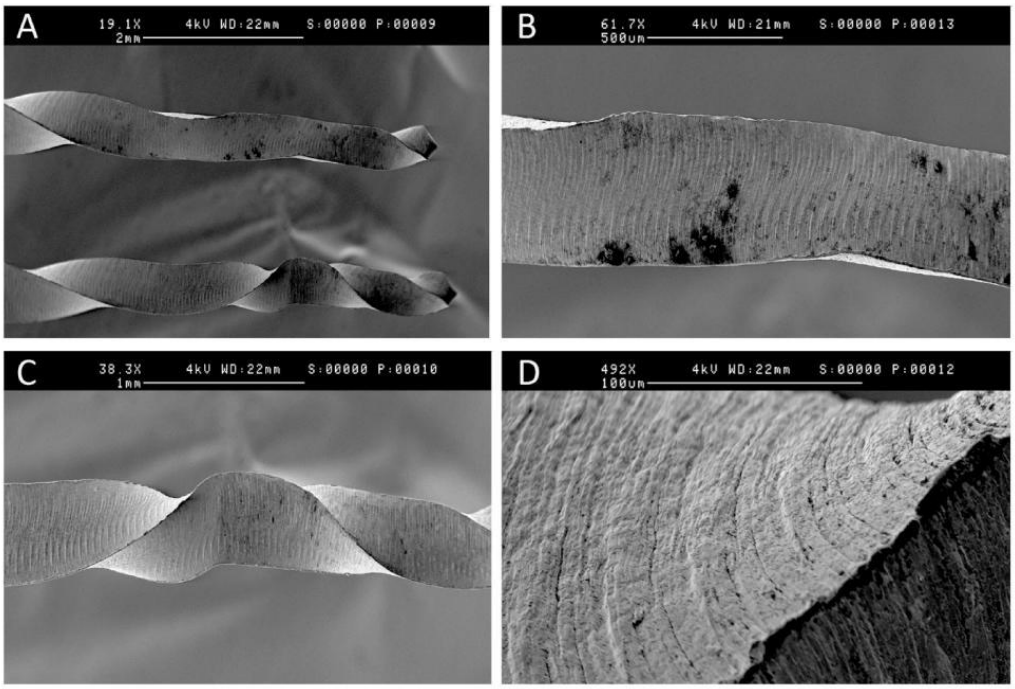

Table 3.2 The time of fatigue life (in seconds) of TYP CM and TYP files (mean ± S. D.) until fracture at a curvature of 40o with a 14 mm radius in water conditions after being exposed to torsional stress at 25%, 50% and 75% preloading of the maximum distortion angle before fracture. Different superscripts letters indicate a statistically significant difference at $P < 0.05$ (post hoc analysis).

Files	Preloading of distortion angles			
	0	25%	50%	57%
TYP 25/.04	852 ± 212a (sec)	317 ± 115b (sec)	483 ± 131bc (sec)	354 ± 93b (sec)
TYP 25/.04	3043 ± 579b (sec)	796 ± 226a (sec)	814 ± 173a (sec)	474 ± 120bc (sec)
TYP 25/.04	184 ± 57b (sec)	235 ± 65b (sec)	254 ± 26b (sec)	184 ± 45 (sec)
TYP CM 40/.04	901 ± 206a (sec)	1070 ± 198 (sec)	524 ± 68c (sec)	429 ± 120c (sec)

Figure 3.12 The time of fatigue life (sec) of TYP CM and TYP files until fracture at a curvature of 40o with a 14 mm radius in water conditions after being exposed to torsional stress at 25%, 50% and 75% preloading of the maximum distortion angle before fracture. Different superscripts indicate statistically significant difference ($P < 0.05$).

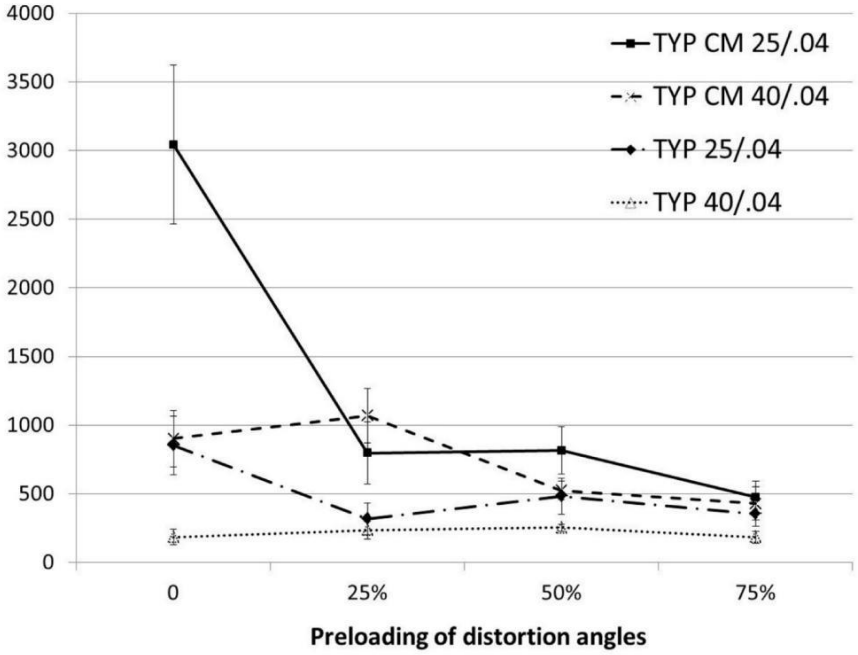

Figure 3.13 Fracture surfaces of size 25 TYP (A & B) and TYP CM (C & D) files after fatigue failure without torsional preloading.

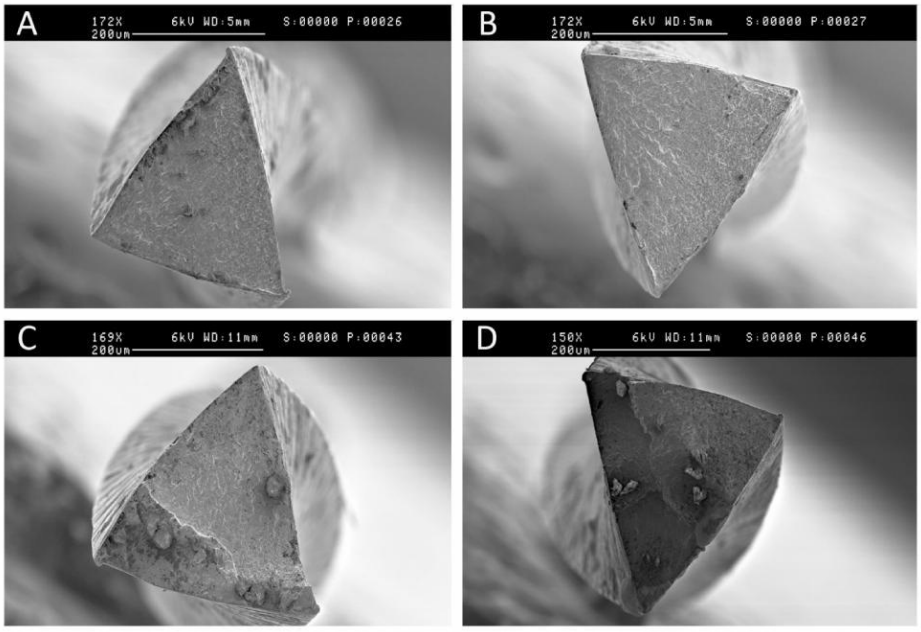

Figure 3.14 Fracture surfaces of size 25 TYP files after fatigue failure with 25% preloading of the maximum distortion angle.

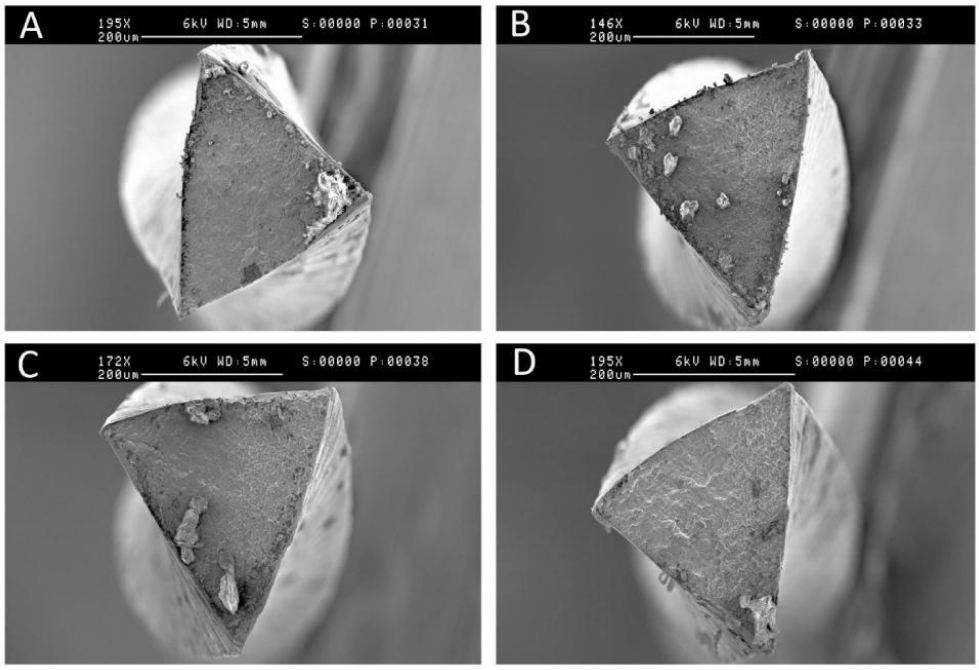

Figure 3.15 Fracture surfaces of size 25 TYP CM files after fatigue failure with 25% preloading of the maximum distortion angle.

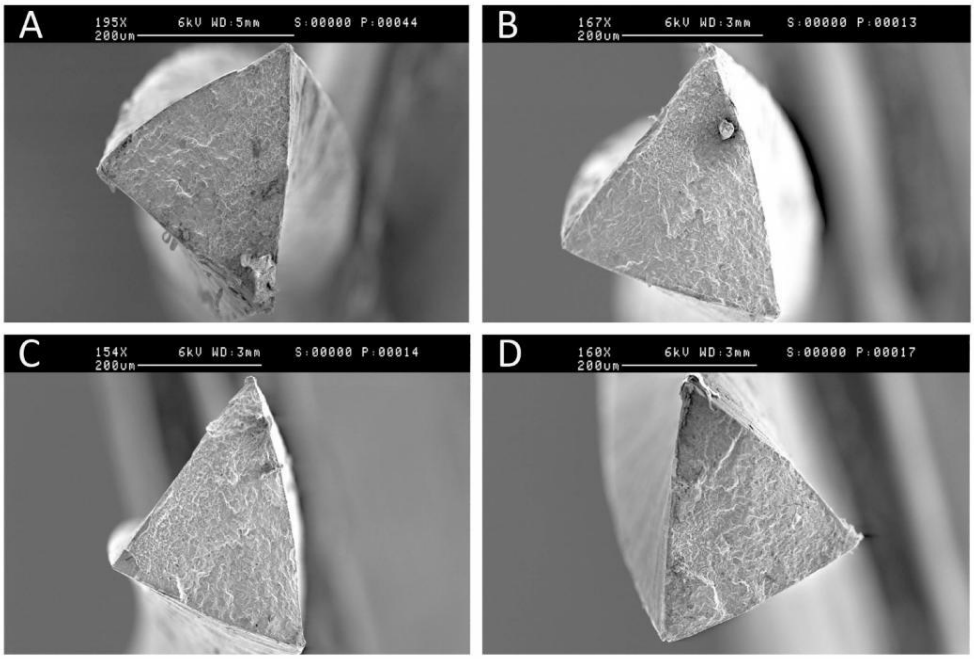

Figure 3.16 Fracture surfaces of size 40 TYP (A & B) and TYP CM (C & D) files after fatigue failure without preloading.

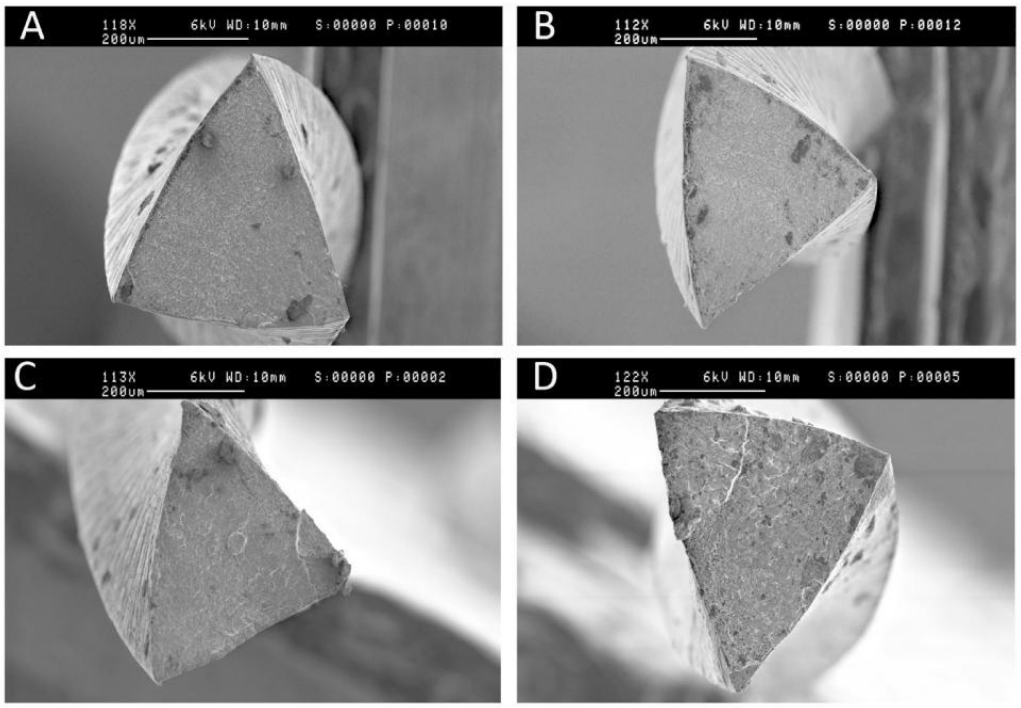

Figure 3.17 Fracture surfaces of size 40 TYP (A & B) and TYP CM (C & D) files after fatigue failure with 25% preloading of the maximum distortion angle.

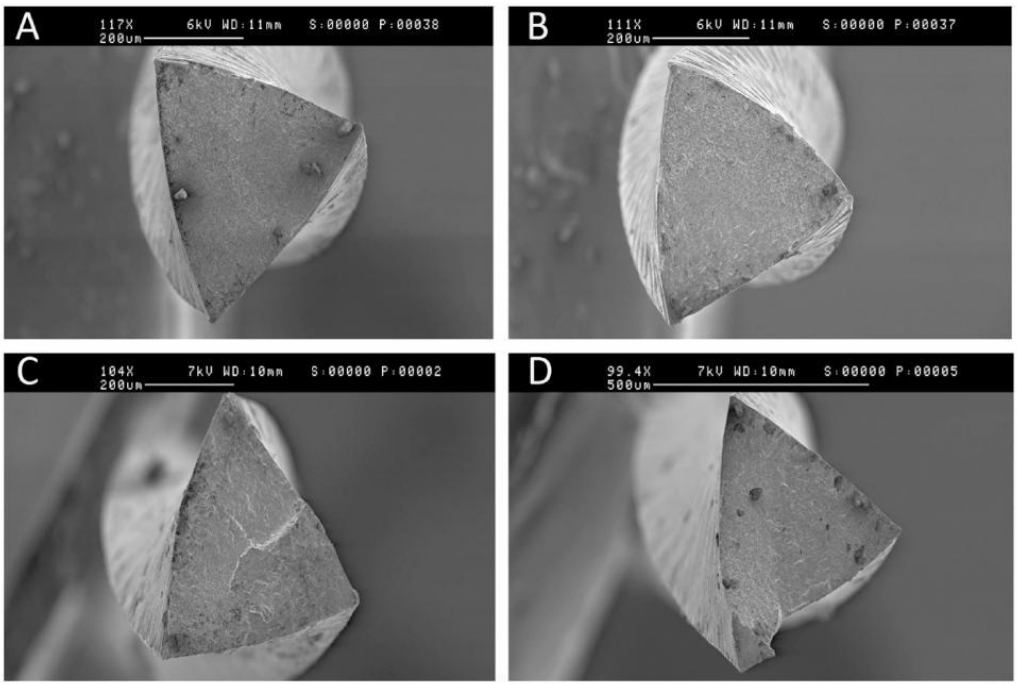

Figure 3.18 Fracture surfaces of size 25 TYP (A & B) and TYP CM (C & D) files after fatigue failure with 50% preloading of the maximum distortion angle.

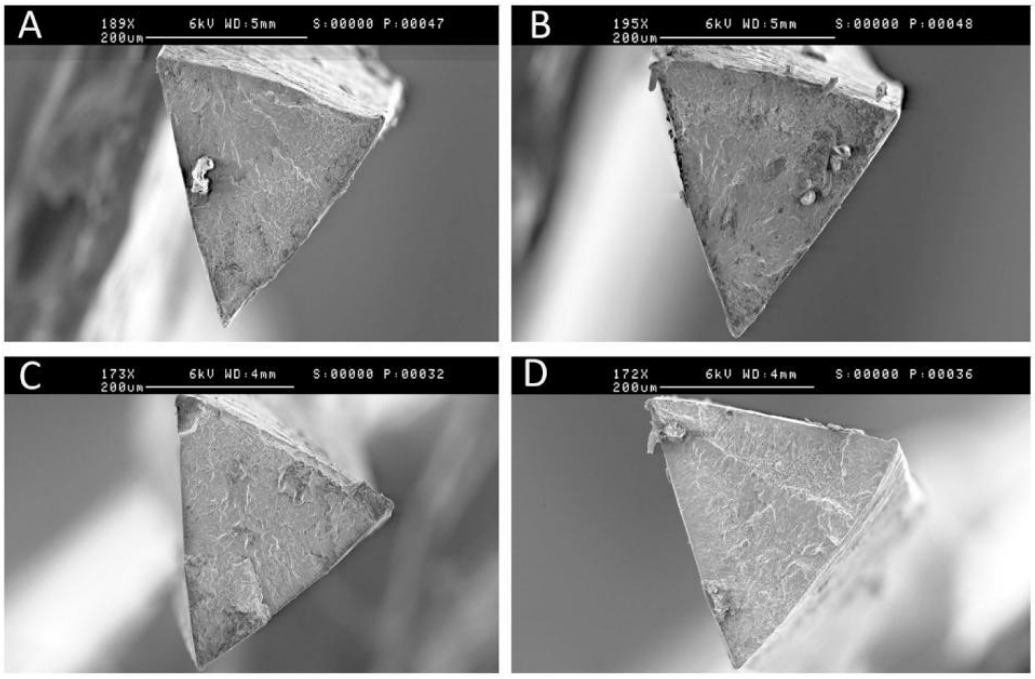

Figure 3.19 Fracture surfaces of size 40 TYP (A & B) and TYP CM (C & D) files after fatigue failure with 50% preloading of the maximum distortion angle.

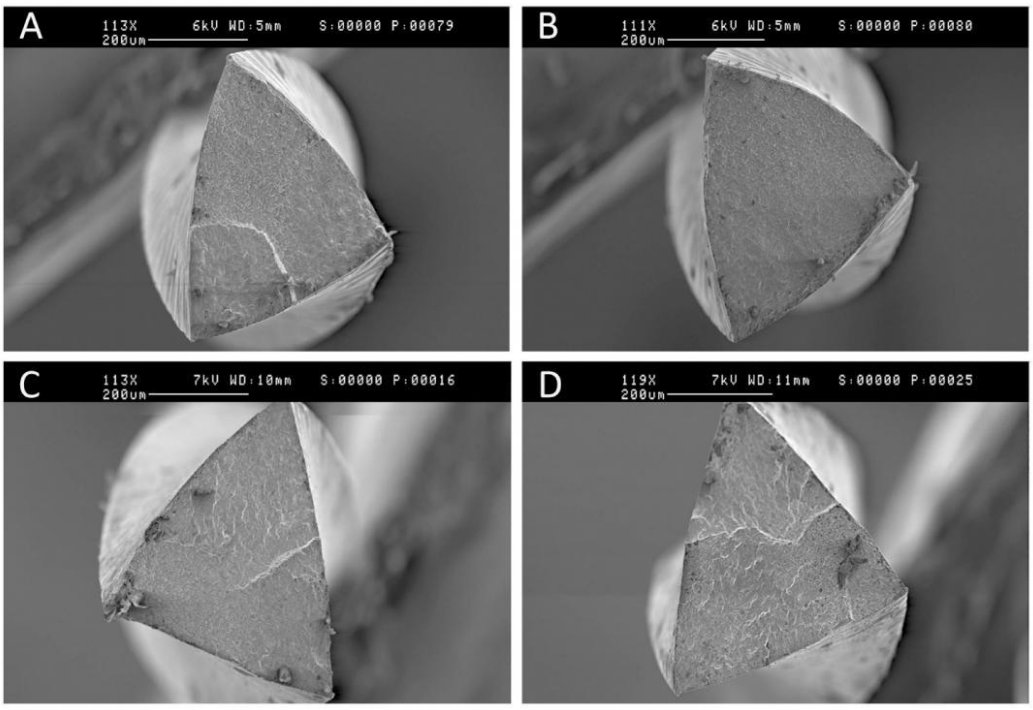

Figure 3.20 Fracture surfaces of size 25 TYP (A & B) and TYP CM (C & D) files after fatigue failure with 75% preloading of the maximum distortion angle.

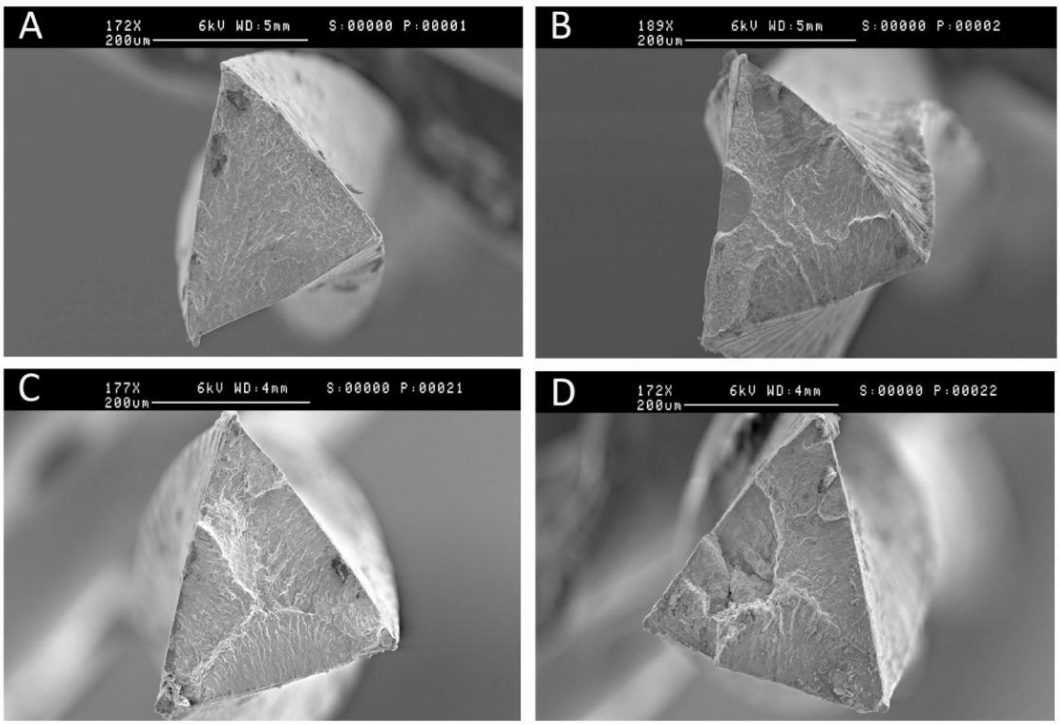

Figure 3.21 Fracture surfaces of size 40 TYP (A & B) and TYP CM (C & D) files after fatigue failure with 75% preloading of the maximum distortion angle.

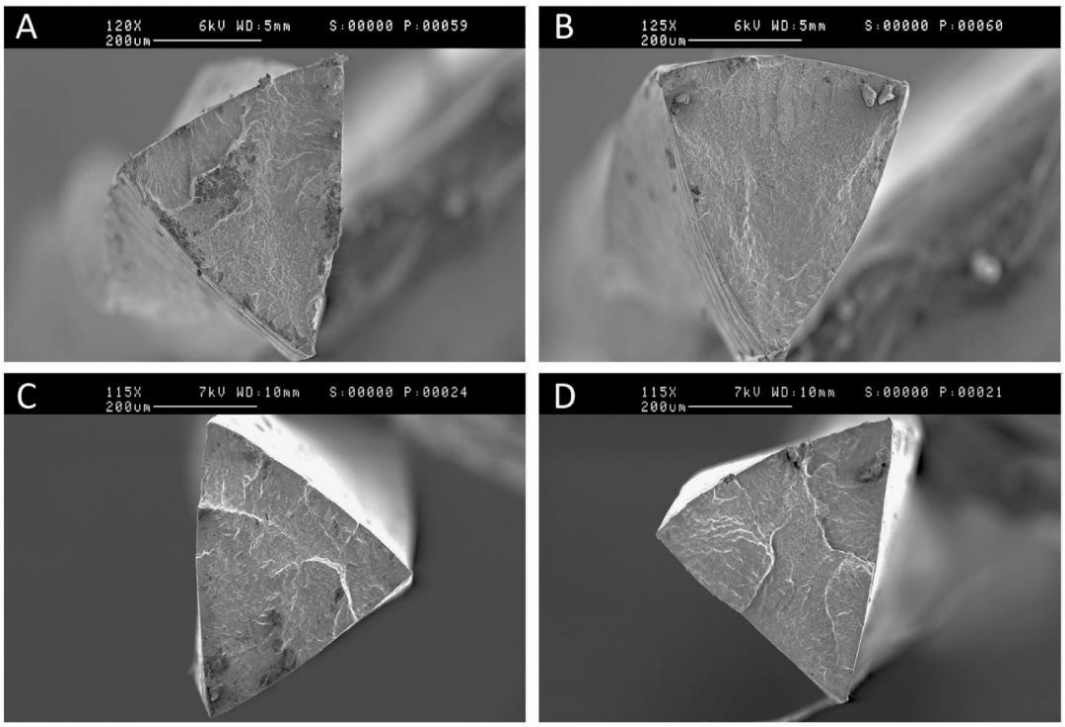

Figure 3.22 Fracture surfaces of size 40 TYP (A) and TYP CM (B) instruments after separation by fatigue with the region of fatigue crack propagation and dimple area outlined (dotted line).

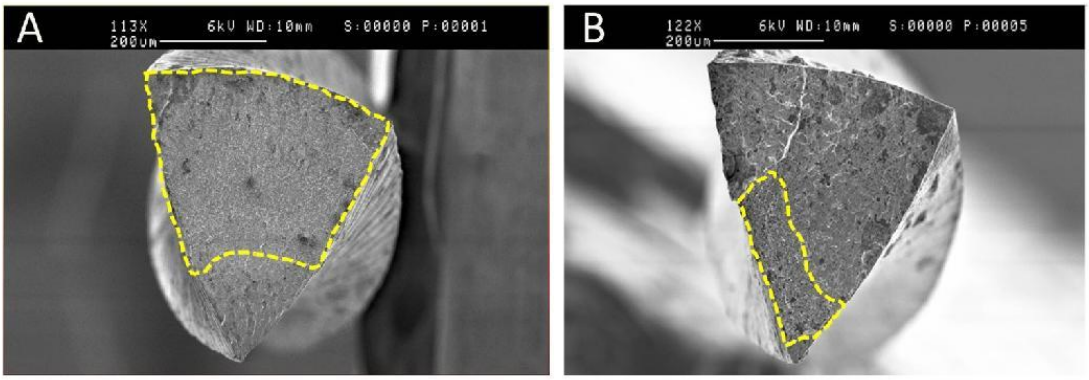

Figure 3.23 Fracture surfaces of size 40 TYP (A) and TYP CM (D) instruments after separation due to fatigue with the region of fatigue crack propagation and dimple area outlined (dotted line); TYP after fatigue failure with 25% (B) and 75% (C) preloading of the maximum distortion angle; TYP CM after fatigue failure with 25% (E) and 75% (F) preloading of the maximum distortion angle.

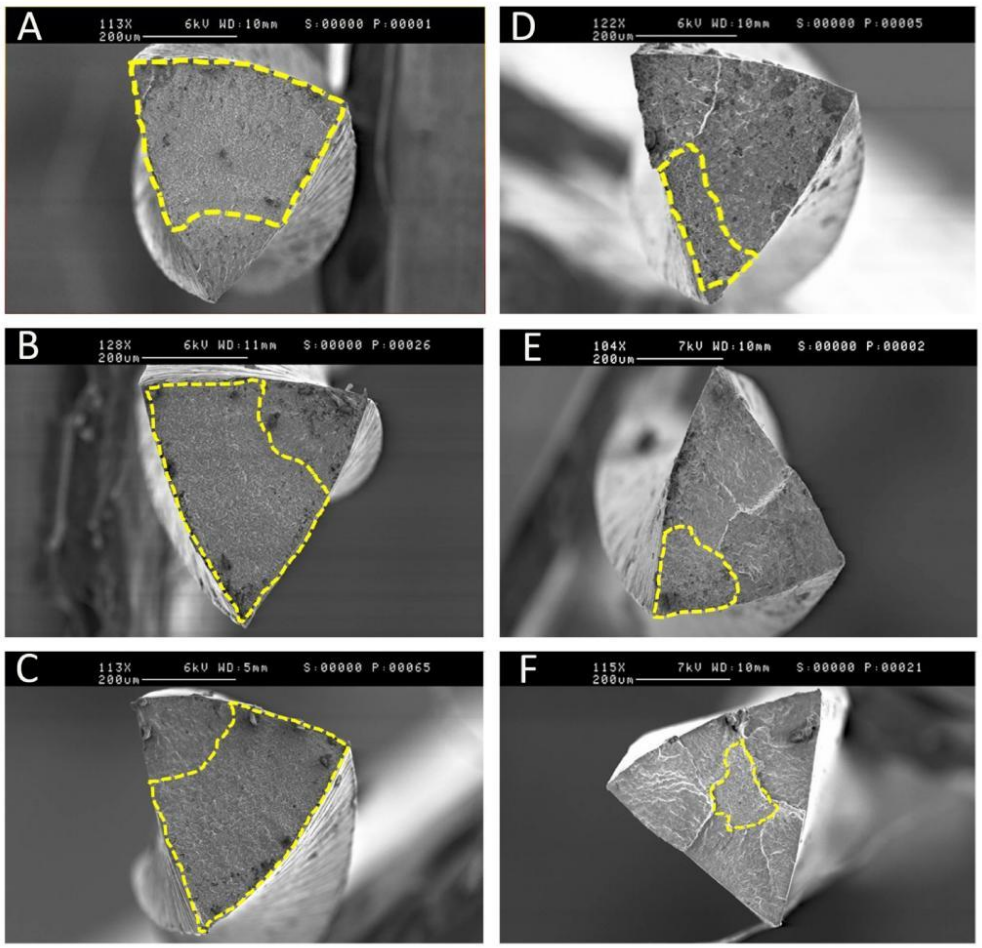

Figure 3.24 Fracture surfaces of size 25 TYP (A) and TYP CM (D) instruments after separation due to fatigue with the region of fatigue crack propagation and dimple area outlined (dotted line); TYP after fatigue failure with 25% (B) and 75% (C) preloading of the maximum distortion angle; TYP CM after fatigue failure with 25% (E) and 75% (F) preloading of the maximum distortion angle.

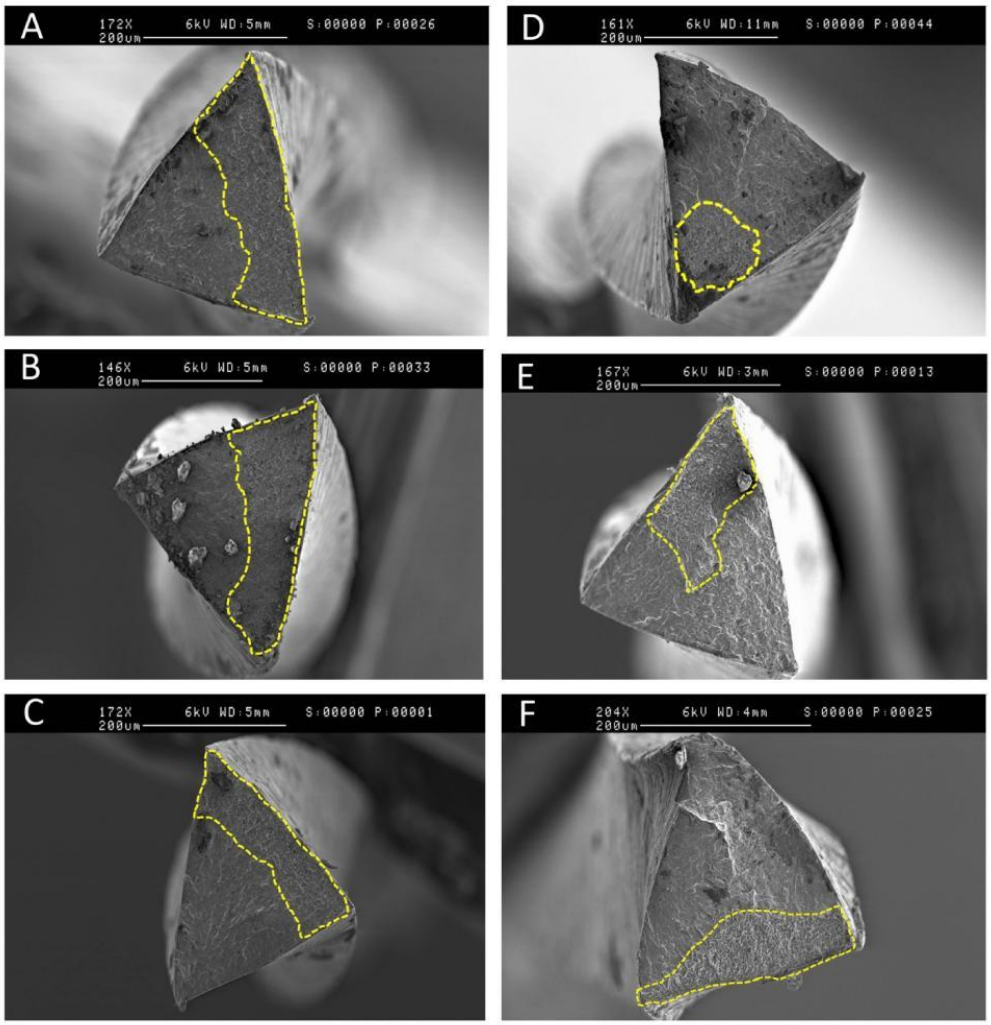

Figure 3.25 Fracture surface after instrument separation due to torque of size 25 TYP (A) and TYP CM (B) files.

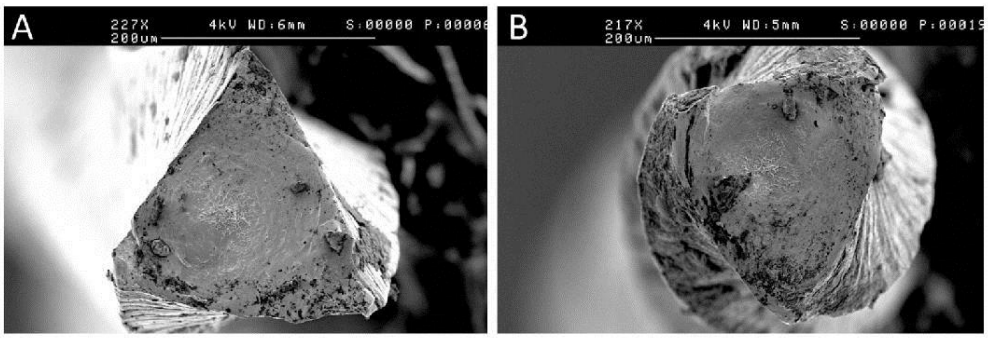

Discussion

Rotational bending and torsional stress will both develop in a rotary instrument during clinical situations. Kim *et al*. (2012) showed that cyclic fatigue had a significant effect on torsional fracture resistance on conventional superelastic ProFile (Dentsply Tulsa Dental) and ProTaper (Dentsply Tulsa Dental) instruments. Later, Cheung *et al*. (2013) studied the effect of torsional preloading on the cyclic fatigue life of ProFile size 25/.06 and ProTaper F1 rotary instruments. Recently, Campbell *et al*. (2014) evaluated the effect of cyclic fatigue on torsional failure of thermomechanically treated TYP CM instruments. The aim of this study was to evaluate the effect of torsional stress preloading angle on fatigue resistance of Typhoon (TYP) CM instruments and TYP instruments of two sizes (25/.04 and 40/.04) in water conditions.

Typhoon CM rotary instruments were recently characterized by a high austenitic finish temperature (Af) of approximately 55oC, indicating that at body temperature, the instrument would contain a significant proportion of martensitic alloy (Shen *et al*. 2011b, Zhou *et al*. 2012). The martensitic form of NiTi has high resistance to fatigue. Therefore, it was not surprising that the TYP CM instruments were more resistant to cyclic fatigue than the TYP instruments both in air and in water. An instrument should be resistant to cyclic fatigue and have sufficient flexibility to permit the preparation of curved systems but also sufficient torque strength so that instrument separation does not occur. As a general rule, while being resistant to cyclic fatigue, flexible instruments have been assumed to be less resistant to torsional load than stiff instruments. Wycoff and Berzins (2012) found that the post-twisting Twisted Files displayed the least amount of torsional stress resistance and the highest angular deflection at fracture compared with traditionally manufactured NiTi files of a similar cross-sectional design. Their findings support the results of the present study where TYP CM files had a higher maximum angular deflection at torsional fracture than instruments made of superelastic NiTi (TYP files).

The influence of previous torsional angular deformation on the flexural fatigue life on conventional NiTi files has also been studied (Galvão *et al*. 2007, Bahia *et al*. 2008). Unused K3 instruments were submitted to a pre-defined rotation before the flexural fatigue test. The results indicated that as the prior angular deformation increases, the number of cycles attained under flexural fatigue condition decreases (Galvão *et al*. 2007). A reduction in the fatigue resistance was registered even with prior torsional loads below the elastic limit of the material (as low as 90° angular deformation). However, Cheung *et al*. (2013) found that the torsional preloads within the superelastic limit of the material may improve the cyclic fatigue resistance of conventional NiTi instruments. The 50% and 75% torsionally preloaded ProFile and all ProTaper files had a higher number of cycles to failure than files without preloading. Comparisons between studies, however, cannot be directly made because different instruments, materials, sample sizes and methodologies were used.

Shen *et al*. (2014) evaluated the effect of and torsional preloading on the cyclic fatigue life of heat-treated size 25/.06 K3XF NiTi instruments. They found that a slight torsional pre-loading reduced the flexural fatigue resistance of K3 and K3XF files. This is in agreement with the present study: the fatigue life of TYP CM and TYP files of size 25/.04 in torsionally preloaded files was lower than in files without preloading, even with as little as 25% torsional preloading. This behavior could be associated with the generation of surface defects during torsional pre-loading, which can act as crack nucleation sites during flexural fatigue. Any residual stress after the torsional preloading may interact with the propagating fatigue crack and manifest as

branching of cracks from the fracture site. It seems that torsional overloads would act in tandem with flexural fatigue to reduce the resistance of NiTi files to failure in clinical situations. However, in large size files (40/.04), despite the previous history of torsional stress application, the fatigue resistance was not affected by the magnitude of the torsional preloads in conventional TYP NiTi instruments; the fatigue resistance of TYP CM files was reduced only after 50% and 75% torsional preloading. In Campbell *et al*. (2014) study, cyclic fatigue was not detrimental to the file's ability to withstand the torsional load of TYP and TYP CM files of size 25/.04. However, in the larger size (40/.04), the 75% preloading TYP instruments had reduced torsional strength; precycling of TYP CM instruments showed slight reduction in the instrument's distortion angle, but there was no correlation with the amount of preloading.

The fatigue life can be expressed as the number of loading cycles required to initiate a fatigue crack and to propagate the crack to a critical size. With continued cyclic loading, the growth of the dominant crack or cracks will continue until the remaining uncracked section of the component no longer can support the load (Cheung *et al*. 2005). At this point, the fracture toughness is exceeded, and the remaining cross-section of the material experiences rapid fracture. This rapid overload fracture is the third stage of fatigue failure, which manifests as the dimple region. The area occupied by the crack growth region (or dimple region) has been previously examined quantitatively (Shen *et al*. 2011a, 2012a, 2014). Theoretically, the continuing reduction in the net area of the remaining intact section because of the progressive propagation of a fatigue crack would lower the load-bearing capacity of the part to such an extent that it fractures in the next load cycle as a result of simple overload. In the present study, the relative sizes of the fractioned areas occupied by the dimple region in size 40 TYP CM instruments with and without preloading were significantly smaller than in TYP instruments. One explanation is that the fatigue resistance of size 40 TYP CM files is significantly higher than that of TYP instruments. Interestingly, the relative size of the dimple area was smaller also in size 25 TYP CM files without preloading than in files with preloading because the fatigue resistance of TYP CM files was 3 - 4 times higher than that of conventional superelastic TYP NiTi files.

Conclusion

The fatigue resistance of TYP CM files was significantly higher than that of TYP files. The size 25 files had a higher fatigue resistance than size 40 files. The angle of rotation at fracture of TYP CM files was significantly higher than that of TYP files. However, while the difference was clear between the two groups (CM and conventional NiTi), there was no significant difference between size 40 and size 25 files within each group. Fatigue resistance of TYP CM and TYP instruments seems to be affected by preloading of distortion angles in the smaller size 25/.04 files, even with a small amount (25%) torsional preloading. However, there was no significant difference in fatigue resistance of size 40 TYP files with and without torsional preloading. TYP CM files of size 40/.04 in the 50% preloading group had a significantly lower fatigue life than the files in the groups with no preloading. The relative size of the fractured area occupied by the dimples was significantly smaller in size 40 TYP CM instruments than in TYP instruments irrespective of preloading. The size of the dimple area was smaller also in size 25 TYP CM files without preloading than in files with preloading.

Acknowledgements

I would like to express my appreciation to the UBC Faculty of Dentistry clinical staff, administration, and my classmates for their support and efforts towards this research. Thank you to both Dr. Haapasalo and Dr. Shen for your research ideas, mentoring and guidance in my research project. Thank you also to Dr. Ya Shen for helping with the statistical analysis. I'd like to thank Dr. Coil who is always there for us, sharing his knowledge and experience. I would also like to thank Dr. Jolanta Aleksejūnienė for being on my committee and the input. She had into making this work successful. My appreciation also goes out to Dr. Les Campell for his help in torsional testing and Dr. Tianfeng Du for her help in SEM imaging.

References

Alapati SB, Brantley WA, Svec TA, Powers JM, Nusstein JM, Daehn GS (2005) SEM observations of nickel-titanium rotary endodontic instruments that fractured during clinical use. *J Endod* 31: 40-3.

ANSI/ADA Specification No. 28. Root canal files and reamers, type K for hand use. Chicago, IL: American Dental Association, 2002.

Bahia MG, Melo MC, Buono VT (2008) Influence of cyclic torsional loading on the fatigue resistance of K3 instruments. *Int Endod J* 10: 883-91.

Cheung GS, Peng B, Bian Z, Shen Y, Darvell BW (2005) Defects in ProTaper S1 instruments after clinical use: fractographic examination. *Int Endod J* 38: 802-9.

Cheung GS, Darvell BW (2007) Low-cycle fatigue of NiTi rotary instruments of various cross-sectional shapes. *Int Endod J* 40: 626-32.

Cheung GS, Shen Y, Darvell BW (2007a) Does electropolishing improve the low-cycle fatigue behavior of a nickel-titanium rotary instrument in hypochlorite? *J Endod* 33: 1217-21.

Cheung GS, Shen Y, Darvell BW (2007b) Effect of environment on low-cycle fatigue of a nickel-titanium instrument. *J Endod* 33: 1433-7.

Cheung GSP (2009) Instrument fracture: mechanisms, removal of fragments, and clinical outcomes. *Endodontic Topics* 16: 1-26.

Cheung GS, Oh SH, Ha JH, Kim SK, Park SH, Kim HC (2013) Effect of torsional loading of nickel-titanium instruments on cyclic fatigue resistance. *J Endod* 39: 1593-7.

Davis JR (2000) ASM specialty handbook: nickel, cobalt, and their alloys. Materials Park, OH: ASM International.

Diemer F, Calas P (2004) Effect of pitch length on the behavior of rotary triple helix root canal instruments. *J Endod* 30: 716-8.

Eggeler G, Hornbogen E, Yawny A, Heckmann A, Wagner M (2004) Structural and functional fatigue of NiTi shape memory alloys. *Mater Sci Eng A* 378: 24-33.

Frick C, Ortega A, Tyber J, Maksound AEIM, maier HJ, Liu Y, Gall K (2005) Thermal processing of polycrystalline NiTi shape memory alloys. *Mater Sci Eng A* 405: 34-49.

Galvão Barbosa FO, Ponciano Gomes JA, Pimenta de Araújo MC (2007) Influence of previous angular deformation on flexural fatigue resistance of K3 nickel–titanium rotary instruments. *J Endod* 33: 1477-80.

Gutmann JL, Gao Y (2012) Alteration in the inherent metallic and surface properties of nickel-titanium root canal instruments to enhance performance, durability and safety: a focused review. *Int Endod J* 45: 113-28.

Hülsmann M, Peters OA, Dummer PMH (2005) Mechanical preparation of root canals: shaping goals, techniques and means. *Endodontic Topics* 10: 30-76.

International Organization for Standardization. Dentistry—Root-canal Instruments—Part 1: General requirements and test methods. ISO 3630–3631, 2008.

Otsuka K, Ren X (2005) Physical metallurgy of Ti-Ni-based shape memory alloys. *Progress in Materials Science* 50, 511-678.

Parashos P, Gordon I, Messer HH (2004) Factors influencing defects of rotary nickeltitanium endodontic instruments after clinical use. *J Endod* 30, 722-5.

Peng B, Shen Y, Cheung GS, Xia TJ (2005) Defects in ProTaper S1 instruments after clinical use: longitudinal examination. *Int Endod J* 38: 550-7.

Peters OA, Gluskin AK, Weiss RA, Han JT (2012) An in vitro assessment of the physical properties of novel Hyflex nickel-titanium rotary instruments. *Int Endod J* 45: 1027-34.

Plotino G, Grande NM, Cordaro M, Testarelli L, Gambarini G (2009) A review of cyclic fatigue testing of nickel-titanium rotary instruments. *J Endod* 35: 1469-76.

Thompson SA (2000) An overview of nickel–titanium alloys used in dentistry. *Int Endod J* 33: 297-310.

Walia HM, Brantley WA, Gerstein H (1988) An initial investigation of the bending and torsional properties of Nitional investigation root canal files. *J Endod* 14: 346-51.

Saburi T (1998) Ti-Ni shape memory alloys. In: Otsuka K, Wayman CM, eds. Shape Memory Materials. Cambridge, UK: Cambridge University Press, pp. 49-96.

Sattapan B, Nervo GJ, Palamara JE, Messer HH (2000) Defects in rotary nickel-titanium files after clinical use. *J Endod* 26:161-5.

Shen Y, Cheung GS, Bian Z, Peng B (2006) Comparison of defects in ProFile and ProTaper systems after clinical use. *J Endod* 32: 61-5.

Shen Y, Qian W, Abtin H, Gao Y, Haapasalo M (2011a) Fatigue testing of controlled memory wire nickel-titanium rotary instruments. *J Endod* 37: 997-1001.

Shen Y, Zhou HM, Zheng YF, Campbell L, Peng B, Haapasalo M (2011b) Metallurgical characterization of controlled memory wire nickel-titanium rotary instruments. *J Endod* 37: 1566-71.

Shen Y, Qian W, Abtin H, Gao Y, Haapasalo M (2012a) Effect of environment on fatigue failure of controlled memory wire nickel-titanium rotary instruments. *J Endod* 38: 376-80.

Shen Y, Cheung GS (2013) Methods and models to study nickel-titanium instruments. *Endodontic Topics* 29: 18-41.

Shen Y, Zhou HM, Zheng YF, Peng B, Haapasalo M (2013a) Current challenges and concepts of the thermomechanical treatment of nickel-titanium instruments. *J Endod* 39: 163-72.

Shen Y, Coil JM, Zhou H, Zheng Y, Haapasalo M (2013b) HyFlex nickel-titanium rotary instruments after clinical use: metallurgical properties. *Intl Endod J* 46: 720-9.

Shen Y, Zhou H, Campbell L, Wang Z, Wang R, Du T, Haapasalo M (2014) Fatigue and nanomechanical properties of K3XF nickel titanium instruments. *Intl Endod J* 40, Feb 13. doi: 10.1111/iej.12265. [Epub ahead of print]

Souter N, Messer HH (2005) Complications associated with fractured file removal using an ultrasonic technique. *J Endod* 31: 450-2.

Spili P, Parashos P, Messer HH (2005) The impact of instrument fracture on outcome of endodontic treatment. *J Endod* 31: 845-50.

Wang FE, Buehler WJ, Pickart SJ (1965) Crystal structure and a unique martensitic transition of TiNi. *J Appl Phys* 36: 3232-9.

Wycoff RC, Berzins DW (2012) An in vitro comparison of torsional stress properties of three different rotary nickel-titanium files with a similar cross-sectional design. *J Endod* 38: 1118- 20.

Wei X, Ling J, Jiang J, Huang X, Liu L (2007) Modes of failure of ProTaper nickel-titanium rotary instruments after clinical use. *J Endod* 33: 276-9.

Zhou HM, Shen Y, Zheng W, Li L, Zheng YF, Haapasalo M (2012) Mechanical properties of controlled memory and superelastic nickel-titanium wires used in the manufacture of rotary endodontic instruments. *J Endod* 38: 1535-40.

Zinelis S, Darabara M, Takase T, Ogane K, Papadimitriou GD (2007) The effect of thermal treatment on the resistance of nickel–titanium rotary files in cyclic fatigue. *Oral Surg Oral Med Oral Pathol Oral Radiol Endod* 103: 843-7.

Zinelis S, Eliades T, Eliades G (2010) A metallurgical characterization of ten endodontic Ni-Ti instruments: assessing the clinical relevance of shape memory and superelastic properties of Ni-Ti endodontic instruments. *Int Endod J* 43: 125-34.